



Pharmacokinetics and effects of tetrabromobisphenol a (TBBPA) to early life stages of zebrafish (*Danio rerio*)



Hongling Liu^a, Zhiyuan Ma^a, Tao Zhang^a, Nanyang Yu^a, Guanyong Su^a, John P. Giesy^{a, b, c}, Hongxia Yu^{a, *}

^a State Key Laboratory of Pollution Control and Resource Reuse, School of the Environment, Nanjing University, Nanjing, Jiangsu 210023, China

^b Toxicology Centre and Department of Veterinary Biomedical Sciences, University of Saskatchewan, Saskatoon, SK S7N 5B3, Canada

^c School of Biological Sciences, University of Hong Kong, China

HIGHLIGHTS

- Five TBBPA metabolites were identified in Zebrafish embryos/larvae or solution.
- TBBPA and metabolites can stably bind to ThR α receptor by molecular docking and MD simulation.
- TBBPA is a dominating potency toxin based on quantitative toxicity assessment.
- Bioaccumulation and metabolism rate of TBBPA are 19.33% and 8.88%, respectively.
- TBBPA can perturb ThR and AR receptor-associated pathways.

ARTICLE INFO

Article history:

Received 3 August 2017

Received in revised form

18 September 2017

Accepted 19 September 2017

Available online 29 September 2017

Handling Editor: David Volz

Keywords:

Kinetics model

Internal dose

Transcriptional co-regulators

Receptor-mediated network

HPLC-MS

ABSTRACT

In silico and *in vivo* approaches were combined in an aggregate exposure pathway (AEP) to assess accumulation and effects of waterborne exposures of early life stages of zebrafish (*Danio rerio*) to tetrabromobisphenol A (TBBPA). Three metabolites, two of which were isomers, were detected in fish. Two additional metabolites were detected in the exposure solution. Based on kinetics modeling, proportions of TBBPA that were bioaccumulated and metabolized were 19.33% and 8.88%, respectively. Effects of TBBPA and its metabolites were predicted by use of *in silico*, surflex-Dock simulations that they were capable of interacting with ThR α and activating associated signaling pathways. TBBPA had a greater toxic contribution than its metabolites did when we evaluated the toxicity of these substances based on the toxicity unit method. The half of the internal lethal dose (ILD₅₀) was 18.33 μ g TBBPA/g at 74 hpf. This finding was further confirmed by changes in expressions of ThR α and other NRs as well as associated genes in their signal pathways. Specifically, exposure to 1.6×10^2 , 3.3×10^2 or 6.5×10^2 μ g TBBPA/L significantly down-regulated expression of ThR α and associated genes, *ncor*, *c1d*, *ncoa2*, *ncoa3*, and *ncoa4*, in the AR pathway and of *er2a* and *er2b* genes in the ER pathway.

© 2017 Elsevier Ltd. All rights reserved.

1. Introduction

2,2',6,6'-Tetrabromo-4,4'-isopropylidenediphenol (Tetrabromobisphenol A; TBBPA) (CAS# 79-94-7) is used primarily as a reactive flame retardant in printed circuit boards and as an additive flame retardant in several types of polymers. Results have demonstrated the ubiquitous presence of TBBPA in lakes, sediment, animal organs and blood (Yang et al., 2012; He et al., 2013; Xu et al.,

2013). Concentrations of TBBPA in fish serum ranged from 0.8 to 5.3 ng/g lipid weight (lw) at an e-waste site. Concentrations of TBBPA in muscle of fish were between 97 and 245 ng/g lw (Zeng et al., 2014). The bioconcentration factor (BCF) of TBBPA for fathead minnow (*Pimephales promelas*) exposed to radiolabeled ¹⁴C-TBBPA for 24 days was 1200 (Stuer-Lauridsen et al., 2007). While based on parent TBBPA in fathead minnow the BCF would be 160–180 (EU RAR., 2008). Hence, if biotransformation is not considered, bioaccumulation of TBBPA could be overestimated (Gomez et al., 2010). In addition, most studies of biotransformation of TBBPA have been conducted in mammals or amphibians, with the main metabolites identified being sulfate and glucuronide

* Corresponding author.

E-mail address: yuhx@nju.edu.cn (H. Yu).

conjugates of hydroxylated metabolites of TBBPA (Schauer et al., 2006; Knudsen et al., 2007). To date, information on bioaccumulation and biotransformation of TBBPA by aquatic species, especially in the early stages of teleost, is limited. Furthermore, bioavailability of TBBPA to early life stages of fishes is still unclear and there is no direct information on toxic potencies or mechanisms of action of biotransformation products.

Since the chemical structure of TBBPA is similar to that of the active form of thyroid hormones (TH), tri-iodothyronine (T3) and tetra-iodothyronine (T4), concern has been raised about its potential to cause adverse effects on TH functioning in wildlife and humans. In all vertebrates, TH is important for normal development, growth, and metabolism and plays a major role in neurogenesis and functioning of the brain (Zoeller et al., 2002; Bernal, 2007). Results of *in vitro* and *in vivo* studies have demonstrated that TBBPA can disrupt signal transduction pathways (Kitamura et al., 2002; Fini et al., 2012; Zhang et al., 2014; Baumann et al., 2016). For example, TBBPA inhibited binding of T3 to the plasma carrier protein, transthyretin (TTR) at concentrations ranging from 1×10^{-6} to 1×10^{-4} M, enhanced proliferation of rat pituitary GH3 cells and MtT/E-2 cells, and stimulated production of growth hormone (Kitamura et al., 2002). TBBPA can alter circulating concentrations of TH and affect thyroid hormone receptors (ThRs) and act as agonist or antagonist resulting in modulation of transcription in TH transduction pathways in fluorescent transgenic *X. laevis* embryos (Jugan et al., 2010). There are common molecular coding regions in ThRs as well as other nuclear hormone receptors (NRs): the ligand-binding domain (LBD), which can bind ligands with strong affinities, and the DNA-binding domain (DBD), which is involved in recognition of short DNA sequences on target genes (Zhao et al., 2015). Co-repressor and co-activator factors are important co-regulator proteins involved in transcriptional regulation that interact with the LBD of nuclear receptors and regulate transcription of target genes (Zhu et al., 2006; Bertrand et al., 2007; Zhuang et al., 2014). Therefore, changes in transcription of genes related to target, nuclear receptors as well as changes in co-repressor or co-activator can be used to determine receptor-mediated changes.

Objectives of the present study are to assess accumulation and metabolism of TBBPA during embryonic and larval development (6–122 hpf), in zebrafish (*Danio rerio*) as well as changes in expressions of selected genes in the TR pathway. TBBPA and its metabolites are quantified and identified by use of high performance liquid chromatography (HPLC) coupled to a triple quadrupole, tandem mass spectrometer (HPLC-MS/MS). Profiles of metabolites are further investigated by use of HPLC coupled with quadrupole-time-of-flight mass spectrometry (HPLC-Q-TOF-MS). In addition, prediction of binding to the ThR of TBBPA and its metabolites is investigated *in silico* by prediction of docked potency (molecular dynamics simulations). In order to gain a more comprehensive understanding of the perturbation on core NRs mediated signaling networks by TBBPA, expressions of mRNAs for genes of nuclear receptors (e.g. ThR, estrogen (ER), androgen (AR), and aryl hydrocarbon receptors (AhR)) pathways are determined by quantitative real-time polymerase chain reaction (qRT-PCR).

2. Materials and methods

2.1. Animals and chemical exposure protocol

TBBPA was purchased from J&K Scientific (98%, J&K Scientific Ltd., Beijing, China). Dimethyl sulfoxide (DMSO, Nanjing Chemical Reagent Co., Ltd, Nanjing, China) was used as the cosolvent to prepare stock solutions of TBBPA. To maintain suitable osmolality for embryos, rearing water was made by dissolving 60 mg/L instant

ocean salts in dechlorinated water. Adult zebrafish to be used as F0 parents (4-month old, AB wild-type) were obtained from the Institute of Hydrobiology, Chinese Academy of Sciences (Wuhan, China). A semiautomatic aquaculture system (Zhongkehai Recycling Water Aquaculture System Co., Ltd, Qindao, China) was used to maintain parent fish in treated tap water, which contained no measurable ammonia, chlorine or chloramines. Water was disinfected with UV light. Fish were kept under a 14/10 h light/dark photoperiod. Culture and breeding of parent fish as well as subsequent toxicity tests were performed according to OECD Guidelines 210 (OECD, 1992).

Exposures consisted of two types. The first exposure investigated effects of TBBPA on morphology and expressions of mRNA of genes related to ThR, ER, AR, and AhR receptors. A benchmark-dosing regimen was applied using gradient concentrations of TBBPA (0.15, 0.3, 0.6, 1.2, 2.4 and 4.8 μ M corresponding to 8.2×10^1 , 1.6×10^2 , 3.3×10^2 , 6.5×10^2 , 1.3×10^3 and 2.6×10^3 μ g/L) and prepared by rearing water with DMSO (less than 0.1% in exposure medium). Twenty embryos (2 hpf) were randomly selected and placed into 25 mL glass beakers, which contained 20 mL TBBPA exposure solution or vehicle control (DMSO 0.1%). Experiments were performed as previously described (Liu et al., 2015). In briefly, each beaker were contained 10 mL TBOEP in triplicate. Exposures were conducted in an incubator and maintained a stable environment over the course of the experiment (photoperiod: 14/10 h light/dark; static; temperature: 27 ± 1 °C). The fish sample were collected after termination of the experiment (122 hpf) and stored in RNAlater solution (Qiagen Co., Ltd, Germany) at -20 °C until RNA isolation. A second exposure was conducted to investigate bioaccumulation, elimination and metabolism of TBBPA during early life stages (2–122 hpf) of zebrafish. Based on mortality observed during the first exposure, a single test concentration of TBBPA (1.2 μ M, equivalent to 6.5×10^2 μ g/L, which is approximately the LC₃₀ at 98 hpf) with three replicates was selected for quantification of TBBPA and metabolites. In order to have sufficient numbers of samples for quantification of TBBPA and identification of metabolites of TBBPA, 400 embryos were randomly selected and placed into a 150 mL glass culture dish with 100 mL TBBPA exposure solution. The experimental conditions were consistent with the experiment 1. At each sampling period (2, 8, 14, 26, 50, 74, 98 and 122 hpf), exposure water and embryos/larvae were collected (1 mL water sample and 15 biota sample) in triplicate to ensure reproducibility. Embryos/larvae were further rinsed three times in Milli-Q water and storage at -80 °C until further quantification.

2.2. Sample preparation, quantification of internal dose and identification of metabolites

All analyses were carried out at the State Key Laboratory of Pollution Control and Resource Reuse at Nanjing University. Quantification of TBBPA in exposure solutions and embryos/larvae were determined by use of an Agilent 1260 Series system (Agilent Technologies, Palo Alto, CA, USA), equipped with reverse-phase XBridge BEH C18 analytical column of 2.1 mm \times 50 mm and 2.5 μ m particle size (Waters Corporation, Milford, MA, USA) interfaced to a 4000 QTRAP (AB SCIEX, Foster City, CA, USA) with an electrospray ionization (ESI) Turbo V™ Ion Source in negative mode. Identification of TBBPA metabolites was accomplished by use of an Agilent 1260 Series system (Agilent Technologies, Palo Alto, CA, USA), using ACQUITY BEH C18 column (2.1 mm \times 50 mm, 2.6 μ m; Waters, Milford, MA, USA) connected to a Triple TOF 5600 (AB SCIEX, Foster City, CA, USA). Details of procedures are given in the Supporting Information (SI, Text S1).

2.3. Quality assurance and quality control (QA&QC)

Performance of the method was assessed by analyzing spiked samples of water or fish tissue ($n = 6$); recoveries ranged from 88 to 105% and precision, indicated by the relative standard derivation (RSD) was <20%. During the analyses, TBBPA and metabolites were not detectable in any of blanks or controls. The limit of detection (LOD) for TBBPA was defined as an injected concentration of TBBPA that can generate a signal peak 3-time higher than instrumental background noise. Thus, in the present study, the LOD of TBBPA was 0.04 ng/mL (exposure solution) and 0.34 ng/g wm in fish tissue, respectively.

2.4. Exposures of early life stages of zebrafish: uptake, depuration, biotransformation kinetics and measurements of internal cumulative dose

TBBPA was accumulated into and depurated from zebrafish. A two compartment, organism model was used that assumed the rate constants for uptake (k_u) [L/(kg h)] and elimination (k_e)/[h] of TBBPA from and to water. Likewise, employing a one-compartment, organism model was used to derive bioaccumulation kinetics of TBBPA by zebrafish larvae. The exponential, depuration model was used to calculate the rate constant for elimination (k_m) into water, and corrected for biotransformation. To simplify the model, it was assumed that metabolites were excreted, but not accumulated. The kinetic data analysis used previously published methods (Zhang et al., 2010), details of which are presented in the SI, Text S2.

2.5. Prediction of toxic potency and ThR α receptor docking potencies evaluation

Docking and molecular dynamic (MD) simulations were employed to assess potential of TBBPA or metabolites to bind to the zebrafish ThR α receptor. The methods were performed as previously described (Zhuang et al., 2016; Ding et al., 2017). In briefly, the 3D-structure of TBBPA and its metabolites were initially constructed by the sketch molecular module of the Sybyl 7.3 molecular modeling package (Tripos Inc., St. Louis, MO, USA). Optimum conformation of structure was used in molecular docking. Minimized structures were docked into each apo zebrafish ThRs-LBD, by use of the surflex-Dock program of Sybyl 7.3, and the top Total Score conformation of the ligand was selected as the bioactive conformation. Receptors and ligands were merged to be a complex for MD simulation. The MD simulations were carried out using the GRO-MACS 4 package on an International Business Machines (IBM) Blade cluster system. The CHARMM 27 force field was applied to all structural models using GROMACS 4 and SwissParam (<http://www.swissparam.ch/>). The details and evaluation of our docking process are described in SI Text S3.

We then performed an ecotoxicological (Quantitative) Structure Activity Relationship ((Q)SAR) (ECOSAR, USEPA EPIWIN suit) to predict toxic potency of TBBPA to fish. Furthermore, threshold concentrations were converted to toxic units (TU) (Equation (1)) to compare the toxic potential of these compounds, based on concentrations of TBBPA or metabolites that were measured.

$$\text{Toxicunits(TU)} = \frac{C_{fi}}{\text{PLC}_{50}} \quad (1)$$

where: C_{fi} represents cumulative exposure concentration of TBBPA or metabolites from 2 hpf to 96 hpf; PLC_{50} is the LC_{50} for fish predicted by ECOSAR at 96 hpf.

2.6. Quantitative real-time polymerase chain reaction (qRT-PCR)

Isolation of RNA, reverse transcription and qRT-PCR were performed by use of previously reported methods (Zheng et al., 2012). Expression of mRNA for each target was standardized to the housekeeping gene β -actin (Tang et al., 2007), and changes in mRNA expression of related genes (Ct value) were analyzed by the $\Delta\Delta\text{Ct}$ method (Schmittgen and Livak, 2008). Fold change was calculated as $2^{-\Delta\Delta\text{Ct}}$, amplification efficiency of each primer was examined using LinRegPCR (Version: 2013.1, Amsterdam, Netherlands). Primer sequences of receptor-associated genes were listed in Table S6.

2.7. Statistical analyses

Distance-based redundancy (dbRDA) and correlation analyses were executed in R software version 3.2.3. Statistical analyses processed using GraphPad Prism 6 (GraphPad Software Inc., CA, USA). For each gene involved in ThR, AR, ER or AhR pathways, the Agilent Literature Search application was used to construct a biological interaction network within the Cytoscape software v3.2.1 (Cytoscape Consortium, San Diego, CA, USA) (Liu et al., 2013, 2015; Ma et al., 2015). Either WikiPathways (<http://www.wikipathways.org/>) (Pico et al., 2008) or SABioscience Gene Network Central (<http://www.sabiosciences.com/genenetwork/genenetworkcentral.php>) was used to search for interactions among zebrafish genes of interest as mentioned previously (Liu et al., 2013, 2015). Genes were visualized as part of a network by use of Cytoscape. The model describing kinetics of TBBPA and metabolites in zebrafish was constructed by use of originPro 2016 (version b 9.3.226), R^2 of nonlinear fitting was used to measure the fitting curve. During fitting of functions to data, convergence was determined to be sufficient when the maximum number of iterations reached 400 or the chi-square tolerance value reached 1.00×10^{-9} . The Kolmogorov-Smirnov test was used to evaluate data for normality and Levene's test was used to analyze homogeneity of variance. Statistically significant differences among groups were determined by one-way analysis of variance (ANOVA) followed by Tukey's multiple range tests. A value of $p < 0.05$ was considered statistically significant.

3. Results and discussion

3.1. Bioaccumulation and biotransformation of TBBPA

Details of mass spectral information and time course of TBBPA and metabolites concentrations are given (Tables S1–S4 (SI) and Fig. 1A). These data are used to develop kinetic information to derive the dynamic, uptake and depuration models. Detailed kinetic parameters are also given (Table 1). Three metabolites, hydroxylated 2,6-dibromo-4-isopropyl-phenol (TBBPA-Ph + OH, Ph represents $\text{C}_6\text{H}_3\text{OBr}_2$, 2,6-dibromo-4-isopropyl-phenol) and two isomeric forms of methoxylated 2,6-dibromo-4-isopropyl-phenol (TBBPA-Ph + CH_2OH , Isomeric forms) were identified in zebrafish larvae. Concentrations of these compounds increased from 8 to 14 hpf then did not change (26–74 hpf), followed by rapid decrease from 74 to 122 hpf. This result was consistent with concentrations of TBBPA in zebrafish. However, magnitudes of first-order rate constants for uptake (k_u) among four compounds were: TBBPA-Ph + OH (3.85 L/(kg·h)) > TBBPA (3.02 L/(kg·h)) > TBBPA-Ph + CH_2OH (RT6.92) (2.97 L/(kg·h)) = TBBPA-Ph + CH_2OH (2.97 L/(kg·h)), and the rank of elimination rate constants (k_e) were: TBBPA-Ph + OH ($4.39 \times 10^{-2} \text{ h}^{-1}$) > TBBPA-Ph + CH_2OH (RT6.92) ($3.42 \times 10^{-2} \text{ h}^{-1}$) > TBBPA-Ph + CH_2OH ($3.41 \times 10^{-2} \text{ h}^{-1}$) > TBBPA ($3.06 \times 10^{-2} \text{ h}^{-1}$). Oxidative cleavage of TBBPA (TBBPA-Ph) would reduce the size of

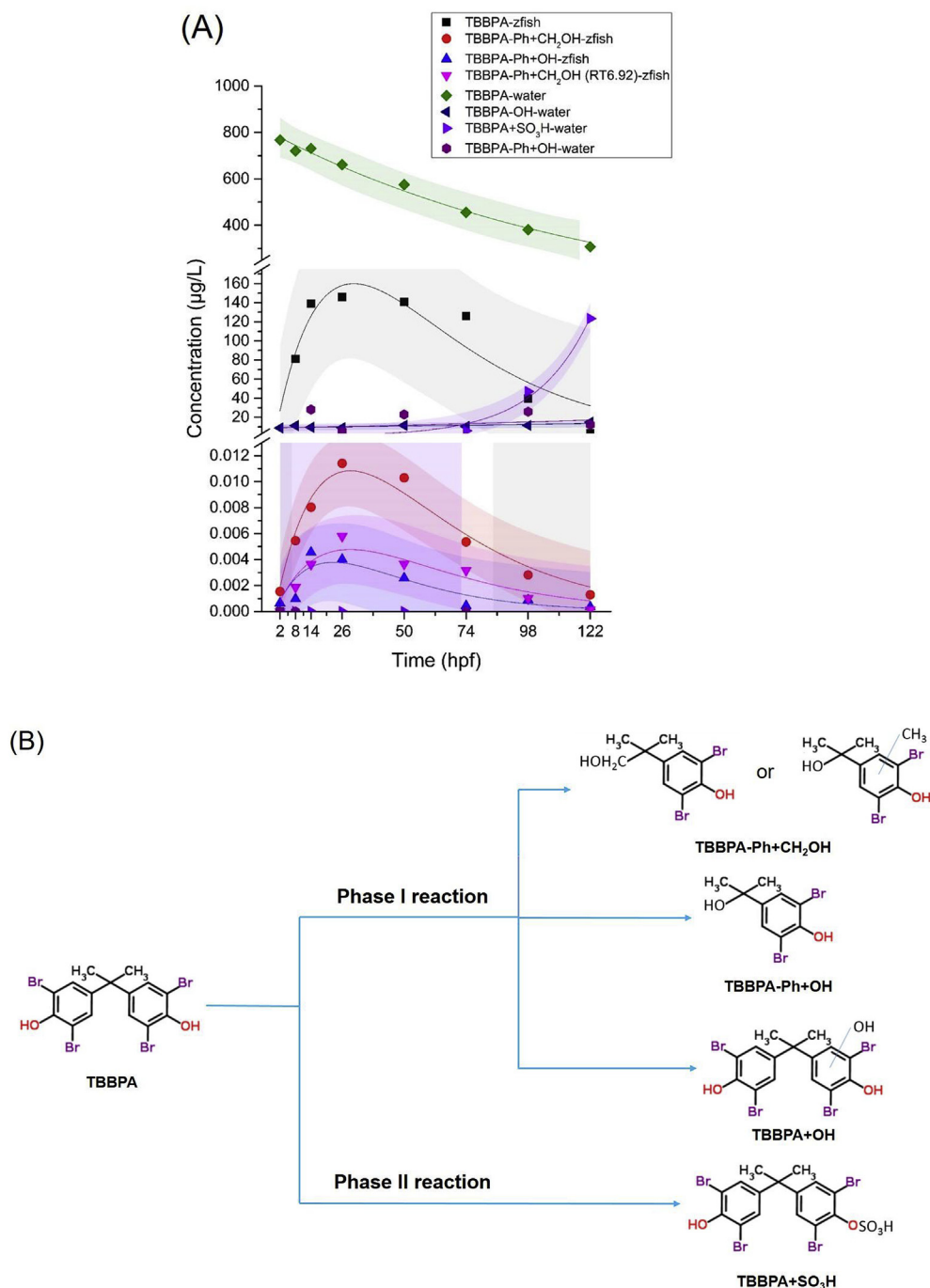


Fig. 1. (A) Measured concentrations of TBBPA and its metabolites in exposure medium ($\mu\text{g/L}$) and in zebrafish embryos/larvae (ng/g , wm). Nonlinear fitting between concentrations in exposure medium and larvae body and time (hpf) are given. Shaded areas represent the 95% confidence intervals (CI). Only detected TBBPA or metabolites were used to construct kinetic model. (B) Structures of TBBPA metabolites and possible metabolic pathways. "Ph" = $\text{C}_6\text{H}_3\text{OBr}_2$.

the compound, which increased the rate of uptake or elimination. In addition, the electron-attracting effect of methoxyl is stronger than that of hydroxyl, because the push effect of the methyl group causes the negative charge of the O atom to be more concentrated. Thus, Hydroxylated (TBBPA-Ph + OH) have a stronger hydrophilicity than methoxylated (TBBPA-Ph + CH₂OH). In contrast, TBBPA had a slower rate of excretion, which means that among these compounds TBBPA had greater bioaccumulate potential. In addition, TBBPA + SO₃H, TBBPA + OH, and TBBPA-Ph + OH were detected in solution. Possible pathways of biotransformation of TBBPA are

shown (Fig. 1B). These compounds were more hydrophilic than those remaining in the body, and are thus less likely to be re-accumulated into zebrafish larvae. The cumulated exposure concentration (CEC) or critical body residues (CBR) from 2 hpf to 122 hpf was derived from kinetic information. The portion of TBBPA accumulated from water was 19.33%, and the proportion biotransformed was 8.88%. This also demonstrated that TBBPA had moderate potential bioaccumulation and biotransformation. This finding is consistent with previous studies in *Xenopus laevis* and Mammals (Fini et al., 2012; Song et al., 2014). Metabolites observed

Table 1
Kinetics model parameters of TBBPA and metabolites to calculate cumulate exposure/residual concentration in water or zebrafish larvae.

Model Type	Compound Name	Compound Class	Detection Medium	Constant Term				BCF(L/kg)	Cumulative Conc (µg/L) ^c				
				F (kg/L) ^b	A	k _u (h ⁻¹)	k _e (h ⁻¹)						
One compartment model	TBBPA	Parent	Zebrafish	1.16 × 10 ⁻²	3.27 × 10 ³	3.50 × 10 ⁻²	3.06 × 10 ⁻²	9.86 × 10 ¹	1.20 × 10 ⁴				
	TBBPA-Ph + CH ₂ OH ^a	Metabolite	Zebrafish	1.16 × 10 ⁻²	3.12 × 10 ²	3.44 × 10 ⁻²	3.41 × 10 ⁻²	8.70 × 10 ¹	7.90 × 10 ⁻¹				
	TBBPA-Ph + CH ₂ OH ^a (RT6.92)	Metabolite	Zebrafish	1.16 × 10 ⁻²	1.78 × 10 ²	3.45 × 10 ⁻²	3.42 × 10 ⁻²	8.70 × 10 ¹	3.47 × 10 ⁻¹				
	TBBPA-Ph + OH ^a	Metabolite	Zebrafish	1.16 × 10 ⁻²	4.99 × 10 ¹	4.47 × 10 ⁻²	4.39 × 10 ⁻²	8.78 × 10 ¹	2.25 × 10 ⁻¹				
Two compartment model	TBBPA	Parent	Water	A ₁	A ₂	a	b	–	6.22 × 10 ⁴				
				5.79 × 10 ²	2.10 × 10 ²	8.21 × 10 ⁻³	5.00 × 10 ⁻³						
Exponential model	TBBPA-OH	Metabolite	Water	A ₃	K _m (h ⁻¹)			–	1.35 × 10 ³				
				9.20	3.15 × 10 ⁻³								
				TBBPA + SO ₃ H	Metabolite	Water	4.18 × 10 ⁻¹			4.67 × 10 ⁻²			2.66 × 10 ³
				TBBPA-Ph + OH ^a	Metabolite	Water	8.98			5.27 × 10 ⁻³			1.52 × 10 ³

^a Ph = C₆H₃OBr₂, 2,6-dibromo-4-isopropyl-phenol.

^b The weight of each juvenile fish is about 0.00077 g, each group has 15 fish, and volume of the water medium is 1 mL.

^c Cumulative residual dose unit (ng/g) in zebrafish larvae have been converted into concentration unit (µg/L).

in zebrafish were also consistent with results of studies of TBBPA in other vertebrates. For example, results of *in vitro* studies of liver microsomes and S9 fraction from crucian carp (*Carassius carassius*) demonstrated that 2,6-dibromo-4-isopropyl-phenol (TBBPA-Ph) was formed by oxidative cleavage of TBBPA, which was assumed to be mediated by phase I, CYP450 monooxygenase enzymes (Zalko et al., 2006; Shen et al., 2012; Zhuang et al., 2017). In another *in vivo* study of rats sulfate and glucuronide forms of TBBPA, which were found in blood plasma, are mediated via phase II metabolic pathways (Hakk et al., 2000; Schauer et al., 2006). Phase I and/or II metabolism are usually considered to be mechanisms of detoxification (Riu et al., 2011a, 2011b).

Effects of chemicals on organisms are a function of rates of accumulation, and transformation as well as rates of damage and repair (National Research Council, 2012). Due to their persistence and potential to be accumulated and toxic potencies, effects of synthetic chemicals need to be evaluated systematically (Hartung, 2009). The National Research Council (NRC) has released two reports, *Toxicity Testing in the 21st Century* (National Research Council, 2007) and *Science and Decisions: Advancing Risk Assessment* (National Research Council, 2009), which substantially advance conceptual and experimental approaches for assessment of hazard and risks of synthetic chemicals. However, toxic potency or modes of action (MoA) of synthetic chemicals especially its metabolites are often difficult. The aggregate exposure pathway (AEP) concept has been envisioned as sequence of key events from sources pathways of external exposure, the biokinetic processes, which result in arriving at target sites of organisms (Teeguarden et al., 2016).

Basal cellular structures and functions are conserved among organisms. Toxic effects are universal among species and tissues (Escher and Hermens, 2002). The AEP can be combined with information on molecular initiating events (MIEs) that cause transductions of signals along adverse outcome pathways (AOPs). The linkage between the AEP and AOP provides an intuitive, natural relationship between exposure and apical responses of individuals to chemical toxicants. Hazard or risks can be estimated by comparing the concentration of the chemical at target organism with the threshold concentration predicted to perturb MIEs and active AOPs. However, concentrations predicted to occur at target sites are difficult to obtain directly. As a surrogate, total concentrations in an organism that elicit a critical effect can be used instead. These are called critical body residues (CBR) or internal effect concentrations (IES). Biotransformation complicates assessment of toxic effects. Thus, to complete assessments of hazards or

risks, it is necessary to apply models of exposure to evaluate or predict bioaccumulation and biotransformation and link those results to the AOP.

Toxic potencies of chemicals can be increased or decreased by metabolism, depending on whether it is activated to bind to a receptor or made easier to excrete (Keskin et al., 2000). Docking studies, that provide conformations of chemicals in proteins, were used to investigate interactions between ligands and receptors and assist with prediction of hydrogen bonds between ligands and proteins (Ghadari et al., 2015; Karaman and Sippl, 2015; Ng et al., 2015). Although a relatively small amount of TBBPA-Ph + OH/CH₂OH accumulated into zebrafish larvae, it could cause toxicological effects if it exceeds the lowest observed effect concentration (LOEC). Affinities of TBBPA metabolites to ligand binding domains (LBDs) of ThRs were investigated by surflex-Dock method (Li et al., 2012). Details of *in silico* analyses were given in Text S2 (SI). Both parent TBBPA and its metabolites were successfully docked into ThR alpha receptor (ThR α) (Fig. T1, SI), which indicates that TBBPA and its metabolites might activate or inhibit the signaling pathway modulated by ThR α . Hence, potential effects of biotransformation products of TBBPA on endocrine function cannot be ignored, and the additive and/or synergistic interactions between TBBPA and its metabolites in fish should be further investigated.

Due to scarcity of data associated with metabolites of TBBPA in aquatic environments, ECOSAR was used to predict potential toxicities of the parent chemical and its metabolites. To compare their toxic potencies including concentrations measured in bodies of zebrafish, TU were employed. Detailed toxicity data and hazard estimations are given in Table S5. The order of potencies (LC₅₀ values at 96 hpf) estimated by use of ECOSAR were of the following rank: TBBPA (0.023 mg/L) > TBBPA + OH (0.046 mg/L) > TBBPA + SO₃H (0.933 mg/L) > TBBPA-Ph + CH₂OH (RT = 6.92; 2.438 mg/L) > TBBPA-Ph + CH₂OH (2.69 mg/L) > TBBPA-Ph + OH (6.078 mg/L). However, based internal doses measured in zebrafish bodies, that accounted for relative bioaccumulations, the order of toxic units were: TBBPA (4.73 × 10⁵) > TBBPA + OH (2.20 × 10⁴) > TBBPA + SO₃H (8.40 × 10²) > TBBPA-Ph + CH₂OH (2.68 × 10⁻¹) > TBBPA-Ph + CH₂OH (RT = 6.92) (1.30 × 10⁻¹) > TBBPA-Ph + OH (3.53 × 10⁻²). Therefore, although both TBBPA and its metabolites have measurable toxic potencies, TBBPA parent had the most significant contribution to TU. External concentrations were converted to internal dose based on the proportion from the medium, which was 19.33%.

3.2. Developmental effects of TBBPA on embryos/larvae of zebrafish

The predominance of untransformed TBBPA in zebrafish larvae, suggested that TBBPA, not its metabolites, most likely resulted in observed adverse outcomes. Before calculation of the threshold for toxic effects the concentration of TBBPA in water (8.20×10^1 , 1.60×10^2 , 3.30×10^2 , 6.50×10^2 , 1.30×10^3 or $2.60 \times 10^3 \mu\text{g/L}$) was converted to a predicted body burden (internal dose, 1.37, 2.67, 5.50, 1.08×10^1 , 2.17×10^1 , or $4.33 \times 10^1 \mu\text{g/g wm}$). Thus, the effects of threshold concentration ($\text{LC}_{50}/\text{EC}_{50}$) can be replaced with the internal lethal/effect dose ($\text{ILD}_{50}/\text{IED}_{50}$). The ILD_{50} was $18.33 \mu\text{g TBBPA/g}$ (Fig. S1) at 74 hpf. Also embryogenesis was delayed in larvae when exposed to 2.60×10^3 , 1.3×10^3 , 6.50×10^2 or $3.3 \times 10^2 \mu\text{g/L}$ at 26 hpf (Fig. 2). The IED_{50} based on delays in development was $26.66 \mu\text{g TBBPA/g}$ (Fig. S2). Likewise, abnormalities, including edema and curvature of the spine, were observed in larvae exposed to 50 hpf. The IED_{50} , based on deformities, was $21.7 \mu\text{g TBBPA/g wm}$ (Fig. S3) and those symptoms did not improve at 74 hpf (Fig. 2). Spinal curvature was also observed at 122 hpf in larvae exposed to $3.30 \times 10^2 \mu\text{g/L}$ or $6.5 \times 10^2 \mu\text{g/L}$.

If kinetics of TBBPA is considered, the body burden of a single zebrafish larva at 26 hpf was $2.88 \mu\text{g/g wm}$ when exposed to $6.50 \times 10^2 \mu\text{g TBBPA/L}$, and this dose did not reach the IED_{50} value

based on delays in development ($26.7 \mu\text{g/g wm}$). However, the delayed development of proliferation of gastrula when exposed to $6.50 \times 10^2 \mu\text{g TBBPA/L}$ at 26 hpf was observed. Early life stages of fish are most sensitive stages and if its development is affected, including morphogenetic movements of cells, involution, convergence, and extension, produced the primary germ layers, various developmental defects can occur. During this sensitive period of development, formation of the gastrula (5–10 hpf) and somite develop, rudiments of the primary organs become visible, the tail bud becomes more prominent and the embryo elongates during the period of segmentation (10–24 hpf) (Kimmel et al., 1995). In the present study, delayed hatching of larvae was observed when exposed to $6.50 \times 10^2 \mu\text{g TBBPA/L}$, which inhibited cellular differentiation at 10 hpf and caused a delay of somites development at 14 hpf, abnormal development, including short tail, delayed hatching and eventually leading to lethality. Therefore, the effects of TBBPA on developmental need to be focused on the earliest stages of embryogenesis and growth-related gene mediated pathways.

3.3. Expressions of genes along pathways modulated by ThR and AR, ER, and AhR

An alternative hypothesis is that TBBPA causes the delayed

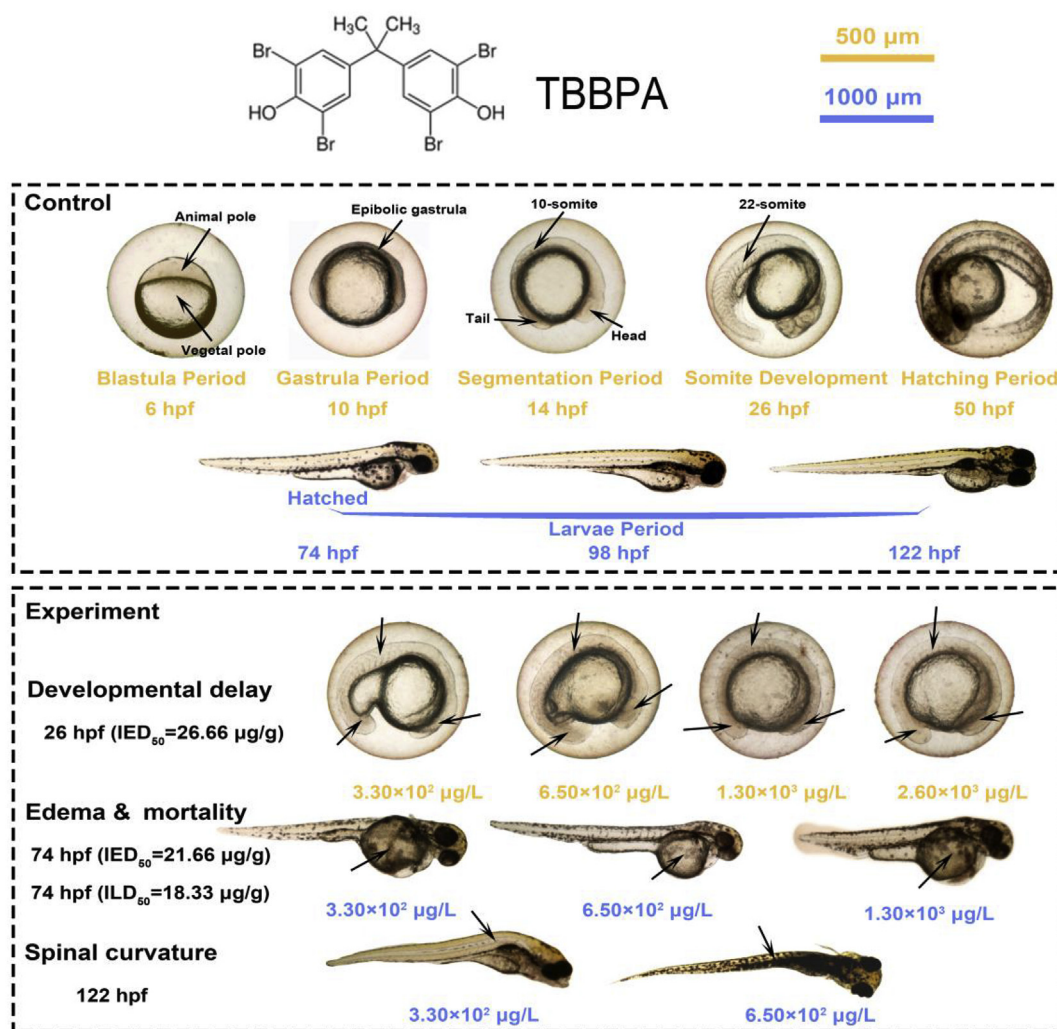


Fig. 2. Photomicrographs of morphologies in control and early life stages of zebrafish exposed to different concentrations of TBBPA. Photos were selected from 3 replicates with $n = 20$ embryos/larvae in each replicate.

growth of zebrafish, leading to endocrine disruption, because its structure is similar to the thyroid hormone. Adverse effects of TBBPA might be caused through alterations of signal transduction pathways mediated by NRs such as ThR mediated signaling pathways. In the present study, qRT-PCR was employed to measure expression of ThR and another three receptors and their related genes (responsible for growth and development) in 122 hpf zebrafish larvae exposed to TBBPA (Table S7). In total, 30 genes that were expressed differently compared with the control group ($p < 0.05$) were detected and quantified. To make the qRT-PCR data more intuitive, dbRDA analyses were conducted (Tang et al., 2013,

2015) to look for overall changes in expressions in zebrafish larvae at 122 hpf to various concentrations of TBBPA (Fig. 3A). The first axis explained 71.64% of total variance, while the second axis explained 21.30%. Significant differences among groups were observed. Ellipses characterized 95% confidence intervals (CI) around group centroids, indicated that if internal dose reached $2.67 \mu\text{g TBBPA/g wm}$ expressions of genes, compared to the control group, could be altered. Changes in expressions of *ccnd1*, *ar*, *er2a* and *er2b* contributed most to the differences among groups (Fig. 3B). All influenced genes were down-regulated and percentages of significant down-regulated (cut-off 1.5-fold) genes were

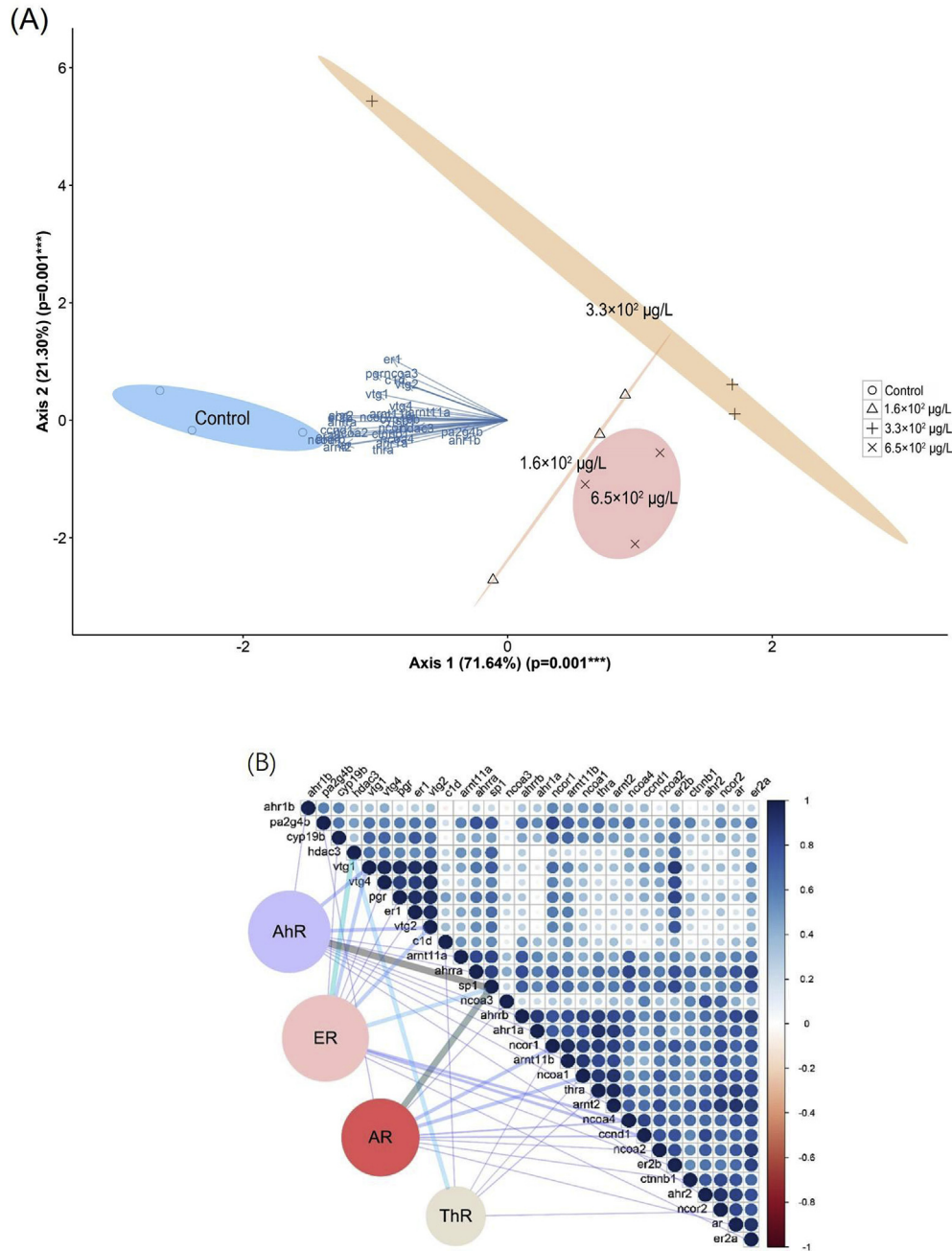


Fig. 3. (A) dbRDA showing changes in receptor-related genes in zebrafish larvae at 122 hpf. Significant differences among groups were observed ($p < 0.05$). Ellipses characterized the 95% CI around group centroids, and the axis accounted for variation while being constrained to explain exposure differences. The genes that contribute most to the dbRDA axes are *ccnd1*, *ar*, *er2a* and *er2b*. (B) Most correlated variables of each gene are given in a data correlogram. The color of the dot shows the strength of the correlation between two variables. In addition, significant regulation of genes among receptors are linked by the line, each edge size represents magnitudes among nuclear receptors and each receptor node size represents the scale of significant regulation. (For interpretation of the references to colour in this figure legend, the reader is referred to the web version of this article.)

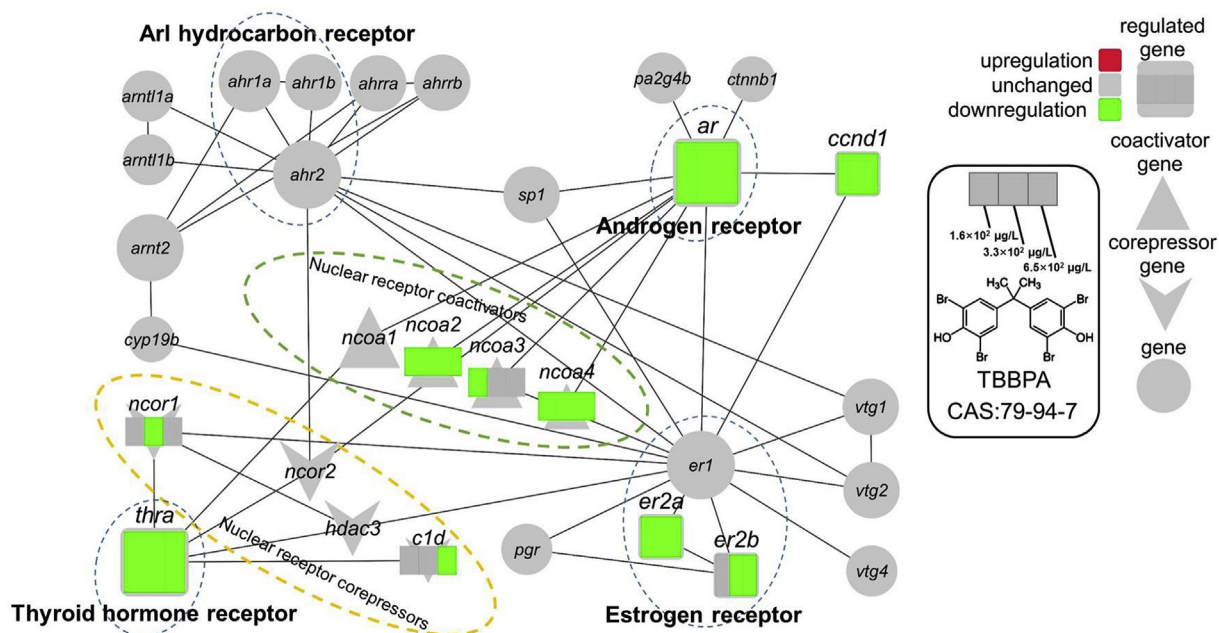


Fig. 4. Core nuclear receptor pathways refer to ThR, AR, ER and AhR of zebrafish. Each node represents a single gene, edges either protein-protein or protein-DNA interactions. The triangle node represents co-activator gene and “V” shape is co-repressor gene. Statistically significant difference ($p < 0.05$, ANOVA) among expression of genes compared to the control group following exposure to various concentrations of TBBPA (1.6×10^2 , 3.3×10^2 and 6.5×10^2 $\mu\text{g/L}$) at 122 hpf are given in respective boxes.

33.3% compared with that of the controls (Fig. 4).

Expressions of genes that mediate ligand-independent transcription repression of thyroid-hormone receptor (co-repressor of NRs) were investigated (Li et al., 2014). TBBPA has been reported to display weak antagonistic activity in human/rat/*Xenopus* ThR α / β (Kojima et al., 2009; Freitas et al., 2011; Otsuka et al., 2014). In eukaryotes, co-repressor first binds to promoter elements (sequence-specific DNA-binding factor) of target NRs, after which it could inhibit transcription of that particular gene product. Transcription is initiated only if there are ligands combined with the LBD as well as the co-repressor (Zhu et al., 2006). In this study, *thra* (thyroid hormone alpha receptor gene) and three related co-repressor genes for thyroid hormone receptor, including *c1d* (C1D nuclear receptor co-repressor), *hdac3* (Histone deacetylase 3) and *ncor1* (Nuclear receptor co-repressor 1) were investigated (Fig. 4). Expressions of *c1d*, *ncor1* and *thra* were significantly down-regulated, and thresholds of internal dose were in the decreasing order of *thra* (2.67 μg TBBPA/g) < *ncor1* (5.50 μg TBBPA/g) < *c1d* (1.08×10^1 μg TBBPA/g). While there were no significant effects on development when the dose reached 2.67 μg TBBPA/g wm, a delay in development was observed when the internal dose reached 5.50 $\mu\text{g/g}$ wm. Expressions of co-repressors might be primarily inhibited and thus affect the pathways.

Coordinated expressions of gene networks in various metabolic, physiological, and developmental processes are mediated by a superfamily of receptors (McKenna and O'Malley, 2002). Previous studies have demonstrated that once steroid ligands bind to an appropriate, NR, the transcription profile of genes involved in these NR pathways could be altered (Liu et al., 2015; Ma et al., 2016). Co-activators are small proteins that interact with NRs to enhance transcription of downstream genes, which are involved in metabolism of lipids and lipoproteins (Bertrand et al., 2007). In the present study, four co-activator genes (*ncoa1*, *ncoa2*, *ncoa3* and *ncoa4*) that are involved in signal transduction pathways of AR, ER and AhR were investigated. Expressions of *ncoa2*, *ncoa3* and *ncoa4* were significantly down-regulated by TBBPA. This indicates that

TBBPA might have antiandrogenic effects.

In fishes, there are three subtypes of the ER (ER1, ER2a and ER2b) (Hawkins et al., 2000; Menuet et al., 2002). These receptors are formed by three distinct genes (*er1*, *er2a* and *er2b*) and can bind to estradiol (E2) with high affinity. In oviparous species, liver is an important target organ for E2. Synthesis of the yolk protein vitellogenin by hepatocyte cells is under control of E2. A previous study demonstrated that exposure to E2 could up-regulate expression of *er1* and down-regulate *er2a*, while *er2b* remained unchanged in liver of zebrafish (Menuet et al., 2004). In the present study, expressions of *er2a* and *er2b* were significantly down-regulated by TBBPA. However, *er1* and related vitellogenin genes (*vtg1*, *vtg2*, *vtg4* and *vtg5*) were not significantly affected. Expression of *vtgs* was not affected by TBBPA, which suggests that TBBPA does not mimic estrogen in zebrafish (Gundel et al., 2007). This result is consistent with results of other *in vivo* studies, showing that levels of *vtgs* were not changed in blood of zebrafish after 21 days exposure to TBBPA (Song et al., 2014).

Two divergent AhRs, AhR1 and AhR2, have been identified and characterized in zebrafish (Andreasen et al., 2002). In the nucleus, when ligands bind to the LBD of the AhR, it dimerizes with aryl hydrocarbon receptor nuclear translocator (ARNT1a, ARNT1b and ARNT2) and aryl hydrocarbon receptor repressor (AHRRA and AHRRB). Association of this heterodimeric complex with specific sequences of DNA (dioxin response elements (enhancers), DREs) could affect expression of downstream genes, such as cytochrome P450-*cyp19b*. (Sutter and Greenlee, 1992; Mimura et al., 1999; Billiard et al., 2006; Aluru et al., 2014). In the present study, no significant changes in expressions of genes in pathways modulated by AhR were observed. TBBPA has been reported to inhibit CYP1A activity (ethoxyresorufin *O*-deethylase, EROD) *in vitro* because TBBPA seemed to compete with the artificial substrate ethoxyresorufin. However, no induction of CYP1A was observed *in vivo* (Ronisz et al., 2004). TBBPA is not a planar molecular and therefore should not be a ligand for the AhR receptor.

4. Conclusion

TBBPA could induce developmental toxicities during early life stage of zebrafish in a concentration-dependent manner. Bioaccumulation of TBBPA was moderate because the rate constant of uptake was greater than that of elimination. The metabolites of TBBPA were more polar than TBBPA and had a strong capability of binding to ThR α . This finding indicates that both TBBPA and its metabolites could alter transcription of genes along ThR-mediated pathways and helps us to understand the mode of action (MOA) *in vivo*. However, considering the amount of the chemical and its metabolites, parent TBBPA is the main contributor of the individual observable effects by using ECOSAR estimation. Therefore, to extend greater understanding of bioaccumulation, distribution, metabolism and elimination (ADME) of TBBPA in aquatic vertebrates, the future study should investigate the sensitivity and power of integrating both *in vivo* and *in silico* approaches with early life stages of fish for elucidating or predicting adverse outcome pathway (AOP) as well as the aggregate exposure pathway (AEP) of emerging chemicals.

Acknowledgements

This work was co-funded by National Natural Science Foundation (Nos. 21677073 and 21377053) of China. Prof. Giesy was supported by the Canada Research Chair program and a Distinguished Visiting Professorship in the School of Biological Sciences of the University of Hong Kong. The numerical calculations in this paper were performed on the IBM Blade cluster system in the High Performance Computing Center (HPCC) of Nanjing University.

Appendix A. Supplementary data

Supplementary data related to this article can be found at <https://doi.org/10.1016/j.chemosphere.2017.09.137>.

References

- Aluru, N., Jenny, M.J., Hahn, M.E., 2014. Knockdown of a zebrafish aryl hydrocarbon receptor repressor (AHRRA) affects expression of genes related to photoreceptor development and hematopoiesis. *Toxicol. Sci.* 139, 381–395.
- Andreasen, E.A., Spitsbergen, J.M., Tanguay, R.L., Stegeman, J.J., Heideman, W., Peterson, R.E., 2002. Tissue-specific expression of AHR2, ARNT2, and CYP1A in zebrafish embryos and larvae: effects of developmental stage and 2,3,7,8-tetrachlorodibenzo-p-dioxin exposure. *Toxicol. Sci.* 68, 403–419.
- Baumann, L., Ros, A., Rehberger, K., Neuhauss, S.C., Segner, H., 2016. Thyroid disruption in zebrafish (*Danio rerio*) larvae: different molecular response patterns lead to impaired eye development and visual functions. *Aquat. Toxicol.* 172, 44–55.
- Bernal, J., 2007. Thyroid hormone receptors in brain development and function. *Nat. Clin. Pract. Endocrinol. Metab.* 3, 249–259.
- Bertrand, S., Thisse, B., Tavares, R., Sachs, L., Chaumot, A., Bardet, P.L., Escriva, H., Duffraisse, M., Marchand, O., Safi, R., Thisse, C., Laudet, V., 2007. Unexpected novel relational links uncovered by extensive developmental profiling of nuclear receptor expression. *Plos Genet.* 3, e188.
- Billiard, S.M., Timme-Laragy, A.R., Wassenberg, D.M., Cockman, C., Di Giulio, R.T., 2006. The role of the aryl hydrocarbon receptor pathway in mediating synergistic developmental toxicity of polycyclic aromatic hydrocarbons to zebrafish. *Toxicol. Sci.* 92, 526–536.
- Ding, K., Kong, X., Wang, J., Lu, L., Zhou, W., Zhan, T., Zhang, C., Zhuang, S., 2017. Side chains of parabens modulate antiandrogenic activity: *in vitro* and molecular docking studies. *Environ. Sci. Technol.* 51, 6452–6460.
- Escher, B.I., Hermens, J.L.M., 2002. Modes of action in ecotoxicology: their role in body burdens, species sensitivity, QSARs, and mixture effects. *Environ. Sci. Technol.* 36, 4201–4217.
- EU RAR, 2008. Risk Assessment of 2, 2', 6, 6' Tetrabromo-isopropylidene Diphenol (Tetrabromobisphenol-a). CAS Number: 79-94-7 EINECS Number: 201-236-9. Final Environmental Draft of February 2008. United Kingdom Environment Agency, Wallingford, Oxfordshire, UK.
- Fini, J.B., Riu, A., Debrauwer, L., Hillenweck, A., Le Mevel, S., Chevolleau, S., Boulahouf, A., Palmier, K., Balaguer, P., Cravedi, J.P., Demeneix, B.A., Zalko, D., 2012. Parallel biotransformation of tetrabromobisphenol A in *Xenopus laevis* and mammals: *Xenopus* as a model for endocrine perturbation studies. *Toxicol. Sci.* 125, 359–367.
- Freitas, J., Cano, P., Craig-Veit, C., Goodson, M.L., Furlow, J.D., Murk, A.J., 2011. Detection of thyroid hormone receptor disruptors by a novel stable *in vitro* reporter gene assay. *Toxicol. Vitro* 25, 257–266.
- Ghadari, R., Alavi, F.S., Zahedi, M., 2015. Evaluation of the effect of the chiral centers of Taxol on binding to beta-tubulin: a docking and molecular dynamics simulation study. *Comput. Biol. Chem.* 56, 33–40.
- Gomez, C.F., Constantine, L., Huggett, D.B., 2010. The influence of gill and liver metabolism on the predicted bioconcentration of three pharmaceuticals in fish. *Chemosphere* 81, 1189–1195.
- Gundel, U., Benndorf, D., von Bergen, M., Altenburger, R., Kuster, E., 2007. Vitellin cleavage products as indicators for toxic stress in zebra fish embryos: a proteomic approach. *Proteomics* 7, 4541–4554.
- Hakk, H., Larsen, G., Bergman, A., Orn, U., 2000. Metabolism, excretion and distribution of the flame retardant tetrabromobisphenol-A in conventional and bile-duct cannulated rats. *Xenobiotica* 30, 831–890.
- Hartung, T., 2009. Toxicology for the twenty-first century. *Nature* 460, 208–212.
- Hawkins, M.B., Thornton, J.W., Crews, D., Skipper, J.K., Dotte, A., Thomas, P., 2000. Identification of a third distinct estrogen receptor and reclassification of estrogen receptors in teleosts. *P Natl. Acad. Sci. U. S. A.* 97, 10751–10756.
- He, M.J., Luo, X.J., Yu, L.H., Wu, J.P., Chen, S.J., Mai, B.X., 2013. Diastereoisomer and enantiomer-specific profiles of hexabromocyclododecane and tetrabromobisphenol A in an aquatic environment in a highly industrialized area, South China: vertical profile, phase partition, and bioaccumulation. *Environ. Pollut.* 179, 105–110.
- Jugan, M.L., Levi, Y., Blondeau, J.P., 2010. Endocrine disruptors and thyroid hormone physiology. *Biochem. Pharmacol.* 79, 939–947.
- Karaman, B., Sippl, W., 2015. Docking and binding free energy calculations of siruin inhibitors. *Eur. J. Med. Chem.* 93, 584–598.
- Keskin, O., Jernigan, R.L., Bahar, I., 2000. Proteins with similar architecture exhibit similar large-scale dynamic behavior. *Biophys. J.* 78, 2093–2106.
- Kimmel, C.B., Ballard, W.W., Kimmel, S.R., Ullmann, B., Schilling, T.F., 1995. Stages of embryonic development of the zebrafish. *Dev. Dyn.* 203, 253–310.
- Kitamura, S., Jinno, N., Ohta, S., Kuroki, H., Fujimoto, N., 2002. Thyroid hormonal activity of the flame retardants tetrabromobisphenol A and tetrachlorobisphenol A. *Biochem. Biophys. Res. Commun.* 293, 554–559.
- Knudsen, G.A., Jacobs, L.M., Kuester, R.K., Sipes, I.G., 2007. Absorption, distribution, metabolism and excretion of intravenously and orally administered tetrabromobisphenol A [2,3-dibromopropyl ether] in male Fischer-344 rats. *Toxicology* 237, 158–167.
- Kojima, H., Takeuchi, S., Uramaru, N., Sugihara, K., Yoshida, T., Kitamura, S., 2009. Nuclear hormone receptor activity of polybrominated diphenyl ethers and their hydroxylated and methoxylated metabolites in transactivation assays using Chinese hamster ovary cells. *Environ. Health Perspect.* 117, 1210–1218.
- Li, J., Li, K., Dong, X., Liang, D., Zhao, Q., 2014. Ncor1 and Ncor2 play essential but distinct roles in zebrafish primitive myelopoiesis. *Dev. Dyn.* 243, 1544–1553.
- Li, X., Ye, L., Wang, X., Wang, X., Liu, H., Qian, X., Zhu, Y., Yu, H., 2012. Molecular docking, molecular dynamics simulation, and structure-based 3D-QSAR studies on estrogenic activity of hydroxylated polychlorinated biphenyls. *Sci. Total Environ.* 441, 230–238.
- Liu, C., Wang, Q., Liang, K., Liu, J., Zhou, B., Zhang, X., Liu, H., Giesy, J.P., Yu, H., 2013. Effects of tris(1,3-dichloro-2-propyl) phosphate and triphenyl phosphate on receptor-associated mRNA expression in zebrafish embryos/larvae. *Aquat. Toxicol.* 128–129, 147–157.
- Liu, H., Tang, S., Zheng, X., Zhu, Y., Ma, Z., Liu, C., Hecker, M., Saunders, D.M., Giesy, J.P., Zhang, X., Yu, H., 2015. Bioaccumulation, biotransformation, and toxicity of BDE-47, 6-OH-BDE-47, and 6-MeO-BDE-47 in early life-stages of zebrafish (*Danio rerio*). *Environ. Sci. Technol.* 49, 1823–1833.
- Ma, Z., Tang, S., Su, G., Miao, Y., Liu, H., Xie, Y., Giesy, J.P., Saunders, D.M., Hecker, M., Yu, H., 2016. Effects of tris (2-butoxyethyl) phosphate (TBOEP) on endocrine axes during development of early life stages of zebrafish (*Danio rerio*). *Chemosphere* 144, 1920–1927.
- Ma, Z., Yu, Y., Tang, S., Liu, H., Su, G., Xie, Y., Giesy, J.P., Hecker, M., Yu, H., 2015. Differential modulation of expression of nuclear receptor mediated genes by tris(2-butoxyethyl) phosphate (TBOEP) on early life stages of zebrafish (*Danio rerio*). *Aquat. Toxicol.* 169, 196–203.
- McKenna, N.J., O'Malley, B.W., 2002. Combinatorial control of gene expression by nuclear receptors and coregulators. *Cell* 108, 465–474.
- Menuet, A., Le Page, Y., Torres, O., Kern, L., Kah, O., Pakdel, F., 2004. Analysis of the estrogen regulation of the zebrafish estrogen receptor (ER) reveals distinct effects of ERalpha, ERbeta1 and ERbeta2. *J. Mol. Endocrinol.* 32, 975–986.
- Menuet, A., Pellegrini, E., Anglade, I., Blaise, O., Laudet, V., Kah, O., Pakdel, F., 2002. Molecular characterization of three estrogen receptor forms in zebrafish: binding characteristics, transactivation properties, and tissue distributions. *Biol. Reprod.* 66, 1881–1892.
- Mimura, J., Ema, M., Sogawa, K., Fujii-Kuriyama, Y., 1999. Identification of a novel mechanism of regulation of Ah (dioxin) receptor function. *Genes Dev.* 13, 20–25.
- National Research Council, 2007. Toxicity Testing in the 21st Century: a Vision and a Strategy. National Academies Press.
- National Research Council, 2009. Science and Decisions: Advancing Risk Assessment. National Academies Press.
- National Research Council, 2012. Exposure Science in the 21st Century: a Vision and a Strategy. National Academies Press.
- Ng, M.C., Fong, S., Siu, S.W., 2015. PSOvina: the hybrid particle swarm optimization

- algorithm for protein-ligand docking. *J. Bioinforma. Comput. Biol.* 13, 1541007.
- OECD, 1992. OECD Guidelines for the Testing of Chemicals. Section 2: Effects on Biotic Systems Test No. 210: Fish, Early-life Stage Toxicity Test. Organization for Economic Cooperation and Development, Paris, France.
- Otsuka, S., Ishihara, A., Yamauchi, K., 2014. Ioxynil and tetrabromobisphenol A suppress thyroid-hormone-induced activation of transcriptional elongation mediated by histone modifications and RNA polymerase II phosphorylation. *Toxicol. Sci.* 138, 290–299.
- Pico, A.R., Kelder, T., van Iersel, M.P., Hanspers, K., Conklin, B.R., Evelo, C., 2008. WikiPathways: pathway editing for the people. *PLoS Biol.* 6 (7).
- Riu, A., Grimaldi, M., Le Maire, A., Bey, G., Phillips, K., Boulahtouf, A., Perdu, E., Zalko, D., Bourguet, W., Balaguer, P., 2011a. Peroxisome proliferator-activated receptor γ is a target for halogenated analogs of bisphenol A. *Environ. Health Perspect.* 119, 1227.
- Riu, A., le Maire, A., Grimaldi, M., Audebert, M., Hillenweck, A., Bourguet, W., Balaguer, P., Zalko, D., 2011b. Characterization of novel ligands of ER α , ER β and PPAR γ : the case of halogenated bisphenol A and their conjugated metabolites. *Toxicol. Sci. Kfr1* 32.
- Ronisz, D., Finne, E.F., Karlsson, H., Forlin, L., 2004. Effects of the brominated flame retardants hexabromocyclododecane (HBCDD), and tetrabromobisphenol A (TBBPA), on hepatic enzymes and other biomarkers in juvenile rainbow trout and feral eelpout. *Aquat. Toxicol.* 69, 229–245.
- Schauer, U.M., Volkel, W., Dekant, W., 2006. Toxicokinetics of tetrabromobisphenol A in humans and rats after oral administration. *Toxicol. Sci.* 91, 49–58.
- Schmittgen, T.D., Livak, K.J., 2008. Analyzing real-time PCR data by the comparative CT method. *Nat. Protoc.* 3, 1101–1108.
- Shen, M., Cheng, J., Wu, R., Zhang, S., Mao, L., Gao, S., 2012. Metabolism of polybrominated diphenyl ethers and tetrabromobisphenol A by fish liver subcellular fractions in vitro. *Aquat. Toxicol.* 114, 73–79.
- Song, M., Liang, D., Liang, Y., Chen, M., Wang, F., Wang, H., Jiang, G., 2014. Assessing developmental toxicity and estrogenic activity of halogenated bisphenol A on zebrafish (*Danio rerio*). *Chemosphere* 112, 275–281.
- Stuer-Lauridsen, F., Cohr, K., Andersen, T.T., 2007. Health and environmental assessment of alternatives to Deca-BDE in electrical and electronic equipment. *Environ. Proj.* 1142, 2007.
- Sutter, T., Greenlee, W., 1992. Classification of members of the Ah gene battery. *Chemosphere* 25, 223–226.
- Tang, R., Dodd, A., Lai, D., McNabb, W.C., Love, D.R., 2007. Validation of zebrafish (*Danio rerio*) reference genes for quantitative real-time RT-PCR normalization. *Acta Biochim. Biophys. Sin.* 39, 384–390.
- Tang, S., Cai, Q., Chibli, H., Allagadda, V., Nadeau, J.L., Mayer, G.D., 2013. Cadmium sulfate and CdTe-quantum dots alter DNA repair in zebrafish (*Danio rerio*) liver cells. *Toxicol. Appl. Pharmacol.* 272, 443–452.
- Tang, S., Wu, Y., Ryan, C.N., Yu, S., Qin, G., Edwards, D.S., Mayer, G.D., 2015. Distinct expression profiles of stress defense and DNA repair genes in *Daphnia pulex* exposed to cadmium, zinc, and quantum dots. *Chemosphere* 120, 92–99.
- Teeguarden, J.G., Tan, Y.M., Edwards, S.W., Leonard, J.A., Anderson, K.A., Corley, R.A., Kile, M.L., Simonich, S.M., Stone, D., Tanguay, R.L., Waters, K.M., Harper, S.L., Williams, D.E., 2016. Completing the link between exposure science and toxicology for improved environmental health decision making: the aggregate exposure pathway framework. *Environ. Sci. Technol.* 50, 4579–4586.
- Xu, J., Zhang, Y., Guo, C., He, Y., Li, L., Meng, W., 2013. Levels and distribution of tetrabromobisphenol A and hexabromocyclododecane in taihu lake, China. *Environ. Toxicol. Chem.* 32, 2249–2255.
- Yang, S., Wang, S., Liu, H., Yan, Z., 2012. Tetrabromobisphenol A: tissue distribution in fish, and seasonal variation in water and sediment of Lake Chaohu, China. *Environ. Sci. Pollut. Res. Int.* 19, 4090–4096.
- Zalko, D., Prouillac, C., Riu, A., Perdu, E., Dolo, L., Jouanin, I., Canlet, C., Debrauwer, L., Cravedi, J.P., 2006. Biotransformation of the flame retardant tetrabromobisphenol A by human and rat sub-cellular liver fractions. *Chemosphere* 64, 318–327.
- Zeng, Y.-H., Luo, X.-J., Zheng, X.-B., Tang, B., Wu, J.-P., Mai, B.-X., 2014. Species-specific bioaccumulation of halogenated organic pollutants and their metabolites in fish serum from an e-waste site, South China. *Arch. Environ. Con. Tox* 67, 348–357.
- Zhang, Y., Huo, M., Zhou, J., Xie, S., 2010. PKSolver: an add-in program for pharmacokinetic and pharmacodynamic data analysis in Microsoft Excel. *Comput. Methods Programs Biomed.* 99, 306–314.
- Zhang, Y.F., Xu, W., Lou, Q.Q., Li, Y.Y., Zhao, Y.X., Wei, W.J., Qin, Z.F., Wang, H.L., Li, J.Z., 2014. Tetrabromobisphenol A disrupts vertebrate development via thyroid hormone signaling pathway in a developmental stage-dependent manner. *Environ. Sci. Technol.* 48, 8227–8234.
- Zhao, Y., Zhang, K., Giesy, J.P., Hu, J., 2015. Families of nuclear receptors in vertebrate models: characteristic and comparative toxicological perspective. *Sci. Rep.* 5, 8554.
- Zheng, X., Zhu, Y., Liu, C., Liu, H., Giesy, J.P., Hecker, M., Lam, M.H., Yu, H., 2012. Accumulation and biotransformation of BDE-47 by zebrafish larvae and teratogenicity and expression of genes along the hypothalamus-pituitary-thyroid axis. *Environ. Sci. Technol.* 46, 12943–12951.
- Zhu, P., Baek, S.H., Bourk, E.M., Ohgi, K.A., Garcia-Bassets, I., Sanjo, H., Akira, S., Kotol, P.F., Glass, C.K., Rosenfeld, M.G., Rose, D.W., 2006. Macrophage/cancer cell interactions mediate hormone resistance by a nuclear receptor derepression pathway. *Cell* 124, 615–629.
- Zhuang, S., Wang, H., Ding, K., Wang, J., Pan, L., Lu, Y., Liu, Q., Zhang, C., 2016. Interactions of benzotriazole UV stabilizers with human serum albumin: atomic insights revealed by biosensors, spectroscopies and molecular dynamics simulations. *Chemosphere* 144, 1050–1059.
- Zhuang, S.L., Lv, X., Pan, L.M., Lu, L.P., Ge, Z.W., Wang, J.Y., Wang, J.P., Liu, J.S., Liu, W.P., Zhang, C.L., 2017. Benzotriazole UV 328 and UV-P showed distinct antiandrogenic activity upon human CYP3A4-mediated biotransformation. *Environ. Pollut.* 220, 616–624.
- Zhuang, S.L., Zhang, C.L., Liu, W.P., 2014. Atomic insights into distinct hormonal activities of bisphenol A analogues toward PPAR γ and α receptors. *Chem. Res. Toxicol.* 27, 1769–1779.
- Zoeller, T.R., Dowling, A.L., Herzig, C.T., Iannacone, E.A., Gauger, K.J., Bansal, R., 2002. Thyroid hormone, brain development, and the environment. *Environ. Health Perspect.* 110 (3), 355–361.

Supporting information

Pharmacokinetics and Effects of Tetrabromobisphenol A (TBBPA) to Early Life Stages of Zebrafish (*Danio rerio*)

Hongling Liu¹, Zhiyuan Ma¹, Tao Zhang¹, Nanyang Yu¹, Guanyong Su¹, John P. Giesy^{1,2,3}, Hongxia Yu^{1*}

¹ State Key Laboratory of Pollution Control and Resource Reuse, School of the Environment, Nanjing University, Nanjing, Jiangsu 210023, China

² Toxicology Centre and Department of Veterinary Biomedical Sciences, University of Saskatchewan, Saskatoon, SK S7N 5B3, Canada

³ School of Biological Sciences, University of Hong Kong, Hong Kong Special Administrative Region, China

Content

Text S1. Sample Preparation and Quantification.	3
Text S2. Uptake, depuration, biotransformation kinetics	6
Text S2. Docking and MD simulations involve in TBBPA and its metabolites to ThR-LBDs protocol <i>in silico</i>.	8
Preparation of structural models	8
Docking and MD simulations	8
Results	9
Figure T1.	10
Table T1.	10
Table T2.	11
Figure S1. S-Curve of mortality at 74 hpf resulted from TBBPA, LC50=2.02 μM (1.1\times10³ μg/L).	12
Figure S2. S-Curve of abnormal head at 26 hpf resulted from TBBPA, EC50=2.94 μM (1.6\times10³ μg/L).	13
Figure S3. S-Curve of abnormalities 50 hpf resulted from TBBPA, LC50=2.38 μM (1.3\times10³ μg/L).	13
Figure S4. The results of the multiple comparisons of ordinary one-way ANOVA.	14
Figure S5. Mass spectrum and secondary spectrum diagram of the parent TBBPA and its metabolites in solution or larvae body at 120 hpf.	16
Table S1. Optimized instrumental parameters, multiple reaction monitoring (MRM; mass-to-charge (m/z)) transitions and limit of quantification (LOQ)) for TBBPA analyzed by liquid chromatography–electrospray ionization (-)-tandem mass spectrometry.	19

Table S2. Raw data of TBBPA in exposure water by HPLC-QTRAP.	20
Table S3. Raw data of TBBPA in zebrafish Embryos /Larvae by HPLC-QTRAP.	22
Table S4. Raw data of TBBPA and metabolites in exposure water and zebrafish body by HPLC-TripleTOF.	24
Table S5. Using ECOSAR to estimate the acute toxicity value (LC50 at 96 hpf) of TBBPA and metabolites.	26
Table S6. Primer Sequences of receptor-associated genes among ThR, AR, ER and AhR receptors for qRT-PCR.	27
Table S7. Fold-change of gene expressions in NR pathways	28

Text S1. Sample Preparation and Quantification.

Homogenated samples of larvae were ground with florisil (Wz. der Floridin Company, USA) followed by accelerated solvent extraction (Dionex ASE 350, Sunnyvale, CA, USA) with 50:50 dichloromethane: hexane (DCM: HEX) at 80 °C and 1500 psi. After moisture removal through sodium sulfate, applying vacuum-rotary evaporation and nitrogen flow procedure to remove solvent of remaining extracts and replaced with 1 mL methanol, and filtered through a 0.46 µm Nylon membrane. The resulting filtrates were transferred to a vial (Agilent Technologies, Santa Clara, CA, USA) for instrumental analyses.

Concentrations of TBBPA in exposure solutions and whole larvae were determined by Agilent 1260 Series system (Agilent Technologies, Palo Alto, CA, USA) equipped with reversed-phase XBridge BEH C18 analytical column of 2.1 mm×50 mm and 2.5 µm particle size (Waters Corporation, Milford, MA, USA) interfaced to a 4000 QTRAP (AB SCIEX, Foster City, CA, USA) with an electrospray ionization (ESI) Turbo VTM Ion Source in negative mode. The HPLC instrumentation consisted of a vacuum degasser, a binary pump, an isocratic pump, and an autosampler. The injector needle was externally washed with methanol prior to any injection. The reversed-phase column was kept at 40 °C during the analysis. The mobile phase consisted of

formic acid 0.1 % in water (A) and methanol (B). Chromatographic gradient elution was the following: constant flow of 0.3 mL/min; 20 % phase B maintained for 0.5 min, then increased up to 70 % B in 2.5 min and maintained at 30 % B for 8.5 min, followed by a linear gradient return to 20% B in 1 min, then maintain for 2.5 min. For detection and quantification of TBBPA by mass spectrometric were performed in the multiple reaction-monitoring mode (MRM) using the most abundant parent and daughter ions for individual TBBPA. The other operation parameters for MS were optimized as follows: gas 1, nitrogen (45 psi); gas 2, nitrogen (55 psi); ion spray voltage, -4500 V; ion source temperature, 550 °C; curtain gas, nitrogen (25 psi). The compound-dependent operation parameters and MRM transitions are listed in Table S1.

Quantification of metabolites of TBBPA were accomplished by use of an Agilent 1260 Series system (Agilent Technologies, Palo Alto, CA, USA), using ACQUITY BEH C18 column (2.1 mm × 50 mm, 2.6 μm, Waters, Milford, MA, USA), connected to a TripleTOF 5600 (AB SCIEX, Foster City, CA, USA). The mobile phase consisted of acetonitrile 5 % in water (A) and methanol (B). The gradient was run as follows: constant flow of 0.4 mL/min; 20 % phase B maintained for 0.5 min, and then increased from 20 % B to 70% B over 7.5 min, followed by a linear rise to 100% B with 1 min and constant for 2 min, then re-equilibrated at 20% B with 1 min, followed by 3 min for equilibration. The mass spectrometer was operated in information dependent acquisition mode (IDA). Gas and other mass spectrometer settings as follows: gas 1, nitrogen (55 psi); gas 2, nitrogen (55 psi); ion spray voltage, 5500V (positive) and -4500 V (negative), respectively; ion source temperature, 550 °C; curtain gas, nitrogen (25 psi). Each cycle consisted of a TOFMS spectrum acquisition for 200 ms (mass range 50–1250 aum).

Concentrations of target compounds in water or larvae were calculated from peak areas (Equations 1 and 2).

$$C_w(\text{ng/mL}) = (A - b)/a \quad (1)$$

$$C_f(\text{ng/g}) = (A - b)/ma \quad (2)$$

Where: C_w is the concentration of compound in water; C_f is the concentration of compound in larvae; A is the peak area of target compound; a is the slope of standard curve; b is intercept of

standard curve; m (g, wet mass) is zebrafish larvae quality.

To characterize bioaccumulation of TBBPA by early life stages of zebrafish, kinetics related to uptake and elimination of TBBPA were investigated. Mean concentrations of TBBPA in exposure solutions collected at 2, 8, 14, 26, 50, 74, 98 and 122 hpf were 7.7×10^2 , 7.2×10^2 , 7.3×10^2 , 6.6×10^2 , 5.8×10^2 , 4.6×10^2 , 3.8×10^2 and 3.1×10^2 $\mu\text{g/L}$ when exposed to single 6.5×10^2 $\mu\text{g TBBPA/L}$, respectively. Correspondingly, mean concentrations of TBBPA in zebrafish larvae collected at the same time points were $<\text{LOD}$ (0.34), 7.0×10^3 , 1.2×10^4 , 1.3×10^4 , 1.2×10^4 , 1.1×10^4 , 3.4×10^3 and 2.9×10^2 ng/g, wm , respectively (Fig. 2A, Tables S2 and S3). Gradual depletion of TBBPA in exposure water was observed during 14-26 hpf ($p < 0.05$) and followed by significant decrease during 26-74 hpf ($p < 0.001$) and back to decrease gradually during 74-122 hpf ($p < 0.05$). In contrast, trends of concentrations of TBBPA in larvae of zebrafish increased significantly from initial stage to 14 hpf ($p < 0.01$) and then did not change significantly during the period of 14 to 74 hpf ($p > 0.05$); Concentrations of TBBPA decreased ($p < 0.0001$) during 74 to 98 hpf then was constant (98-122 hpf, ANOVA, $p > 0.05$) (Fig. S4).

Therefore, determination of overall potency of a compound requires information on potencies of any biotransformation products. By use of HPLC-Q-TOF-MS, several metabolites of TBBPA were identified both in exposure solution and larvae, and their instrumental responses clearly showed an upward trend as a function of duration of exposure (Fig. 2). In the present study, three metabolites, with retention times of 5.45, 5.55 and 7.43 min, respectively were identified in exposure water. Based on MS2 (secondary spectrum diagram) data, three compounds were identified as TBBPA-monosulfate (TBBPA+SO₃H), hydroxylated 2,6-dibromo-4-isopropyl-phenol formed by oxidative cleavage from TBBPA (TBBPA-Ph+OH (Ph=C₆H₃OBr₂)) and TBBPA-hydroxylated (TBBPA+OH) (Table S4 and Fig. S5). Concentrations of metabolites increased gradually but the total remained small relative to concentrations of TBBPA. For residues in zebrafish larvae, three metabolites, including TBBPA oxidative cleavage (hydroxylated 2,6-dibromo-4-isopropyl-phenol (TBBPA-Ph+OH)

and methoxylated two isomeric forms of 2,6-dibromo-4-isopropyl-phenol (TBBPA-Ph+CH₂OH, Isomeric forms), were observed with retention times of 5.55, 6.50 and 6.92 min, respectively.

Text S2. Uptake, depuration, biotransformation kinetics

Functions used to derive rates and rate constants are given (Equation 1), and the solution of the differential equation 1 were listed in equation 2. The bioconcentration factor (BCF) (L/kg) was defined as the ratio of the uptake rate constant k_u [L/(kg h)] and the elimination rate constant k_e [1/h] (Equation 3).

$$\begin{cases} \frac{dC_{\text{water}}}{dt} = -(k_u + k_t)C_{\text{water}} + k_e C_{\text{fish}} \\ \frac{dC_{\text{fish}}}{dt} = k_u C_{\text{water}} - k_e C_{\text{fish}} \\ \frac{dC_{\text{metabolite}}}{dt} = k_m C_{\text{metabolite}} \end{cases} \quad (1)$$

$$\begin{cases} C_{\text{water}} (\mu\text{g/L}) = A_1 e^{-at} + A_2 e^{-bt} \\ C_{\text{fish}} (\text{ng/g}) = A(e^{-k_e t} - e^{-k_u t}) \\ C_{\text{metabolite}} (\mu\text{g/L}) = A_3 e^{k_m t} \end{cases} \quad (2)$$

$$\text{BCF} = \frac{C_f}{C_w} = \frac{k_u}{k_e \square F} \quad (3)$$

Where: C_{water} is the concentration of TBBPA in the exposure solution; C_{fish} is the concentration of TBBPA in larvae; $C_{\text{metabolite}}$ is the concentration of metabolites detected in solution; t represents the time of exposure; k_u represents the rate constant of TBBPA accumulated into zebrafish; k_e represents the rate constant of TBBPA expelled from the fish; k_m represents the rate constant of metabolism; F represents the ratio of the average wet weight of the larvae to the volume of the exposed medium; A , A_1 , A_2 , A_3 , a and b are represented the constant term. Each kinetic equation was integrated as a function of time (From 2 hpf to 122 hpf) to measure cumulative exposure concentration of TBBPA and its metabolites in water and the cumulative residual dose in larvae since the kinetic equations were obtained, The areas will be

calculated (Equation 4).

$$\begin{cases} C_{\text{cumulative-water}} = \int_2^{122} C_{\text{water}}(t) dt \\ C_{\text{cumulative-fish}} = \int_2^{122} C_{\text{fish}}(t) dt \\ C_{\text{cumulative-metabolite}} = \int_2^{122} C_{\text{metabolite}}(t) dt \end{cases} \quad (4)$$

Text S3. Docking and MD simulations involve in TBBPA and its metabolites to ThR-LBDs protocol *in silico*.

Preparation of structural models

The 3D-structure of the TBBPA and metabolites were initially constructed using the sketch molecular module of the Sybyl 7.3 molecular modeling package (Tripos Inc., St. Louis, MO, USA). All hydrogen atoms were added, and the compound geometries were subsequently optimized using a Tripos force field with Gasteiger-Hückel charges, and minimized using the Powell method with a maximum iteration of 1000 to reach an energy convergence gradient value of 0.001 kcal mol⁻¹Å. The minimized structure was used as the initial conformation for molecular docking and MD simulations.

The structural model of the apo form of the zebrafish ThRs-ligand binding domain (LBD) had been built by homology modeling in the SwissModel workspace (<http://swissmodel.expasy.org/workspace/>). The amino acid residue sequence of the ligand binding domain (LBD) of zebrafish ThRs were downloaded from Uniprot (www.uniprot.org), the modeling templates with higher identity and no broken helix were chosen to construct zebrafish ThRs-LBD structures (Table T1). The Ramachandran plots were generated in The Structure Analysis and Verification Server (<http://services.mbi.ucla.edu/SAVES/>) to evaluate the quality of the built zebrafish ThRs, the statistics were shown in Table T2.

Docking and MD simulations

The minimized structures of TBBPA and its metabolites were docked into each apo zebrafish ThRs-LBDs using the surflex-Dock program of Sybyl 7.3, and the top Total Score conformation of ligand was selected as the bioactive conformation. Then the receptors and ligands were merged to be a complex for MD simulation.

The MD simulations were carried out using the GROMACS 4 package on an

International Business Machines (IBM) Blade cluster system. The CHARMM 27 force field was applied to all structural models using GROMACS 4 and SwissParam (<http://www.swissparam.ch/>). The models were solvated in a box with TIP3P water molecules,⁵³ keeping the box boundary at least 10 Å away from any protein atoms. Six sodium ions were subsequently added for charge neutralization. The whole system was energetically minimized by the steepest-descent method,⁵⁴ then the minimized systems were gradually heated from 0 to 300 K at a constant volume for 40 ps with position restraints for ligands. The heated systems at 300 K were equilibrated for 200 ps with position restraints for ligands and for 1 ns without restraints at 1 bar and 300 K. The MD simulations were then performed in the NPT (constant number of particles, pressure and temperature) ensemble with periodic boundary conditions. Electrostatic interactions were calculated using the particle mesh Ewald algorithm and van der Waals interactions were accounted for to a cutoff distance of 10 Å. All simulations were carried out for 10 ns using 2 fs time steps, and snapshots for analysis were saved every 2 ps.

Results

MD simulations were conducted to predict more reliable receptor-ligand interaction mechanisms and to observe the dynamic behavior of ligand in the active site of receptors. The relative RMSD fluctuations for the backbone atoms of TBBPA and its metabolites molecule were less than 0.25 nm after 5 ns, indicating the stability of ligand and LBDs had been reached (Fig. T1.).

Fig. T1. **(A)** Docking of TBBPA and its metabolite ligands to the 3D model of thyroid hormone receptors alpha (ThR α). **(B)** RMSDs of backbones of TBBPA and its metabolites-ThRs complexes during simulation times .

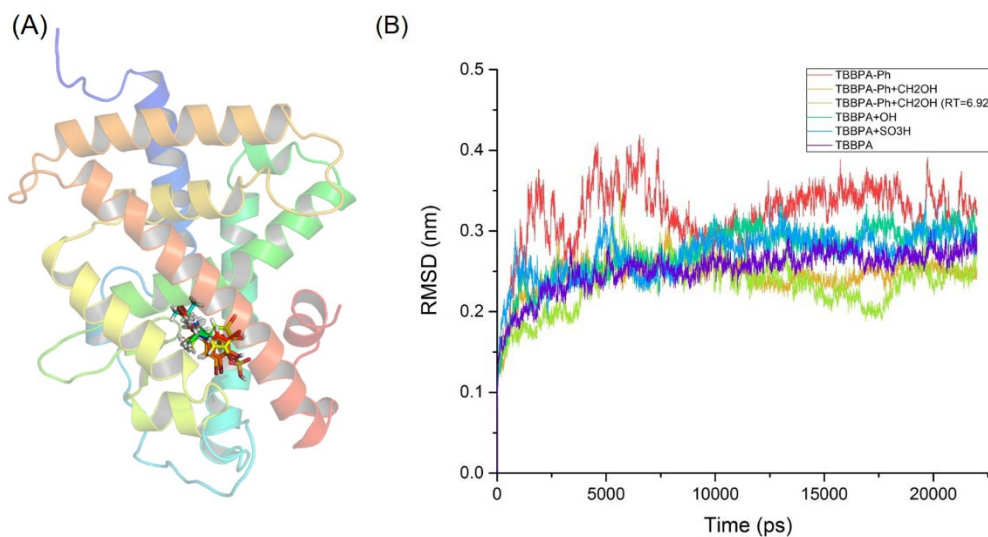


Table T1. Amino acid residue sequence, with template and identities in homology modeling of ThR receptors of zebrafish.

Receptor name	Amino acid residue sequence	Template	Identity (%)
ThR thr α	Q98867	3uvv.1.A	90.16

Table T2. Statistics for Ramachandran Plots. (Data were generated in Ramachandran Plots in the Structure Analysis and Verification Server (<http://services.mbi.ucla.edu/SAVES/>).

Name	Ratio of residues (%)			
	In most favored regions	In additional allowed regions	In generously allowed regions	In disallowed regions
ThR				
<i>thra</i>	91.2	6.6	1.3	0.9

Figure S1. S-Curve of mortality at 74 hpf resulted from TBBPA, $LC_{50}=2.02 \mu\text{M}$ ($1.1 \times 10^3 \mu\text{g/L}$), Transformation of the internal dose was $18.33 \mu\text{g/g}$.

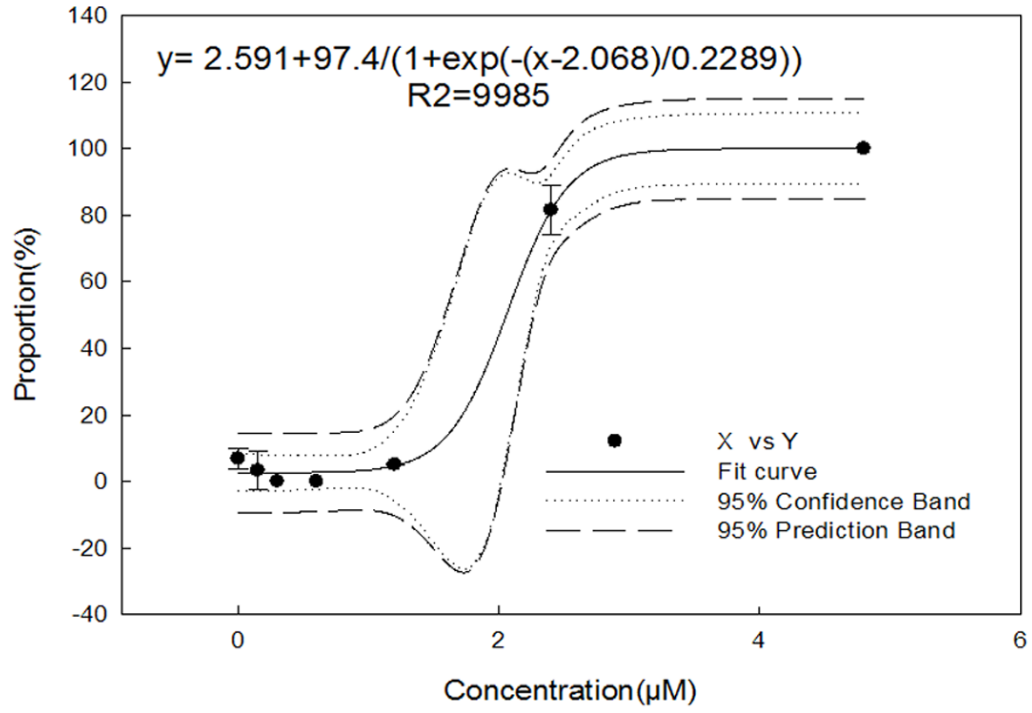


Figure S2. S-Curve of abnormal head at 26 hpf resulted from TBBPA, $EC_{50}=2.94 \mu\text{M}$ ($1.6 \times 10^3 \mu\text{g/L}$), Transformation of the internal dose was $26.66 \mu\text{g/g}$.

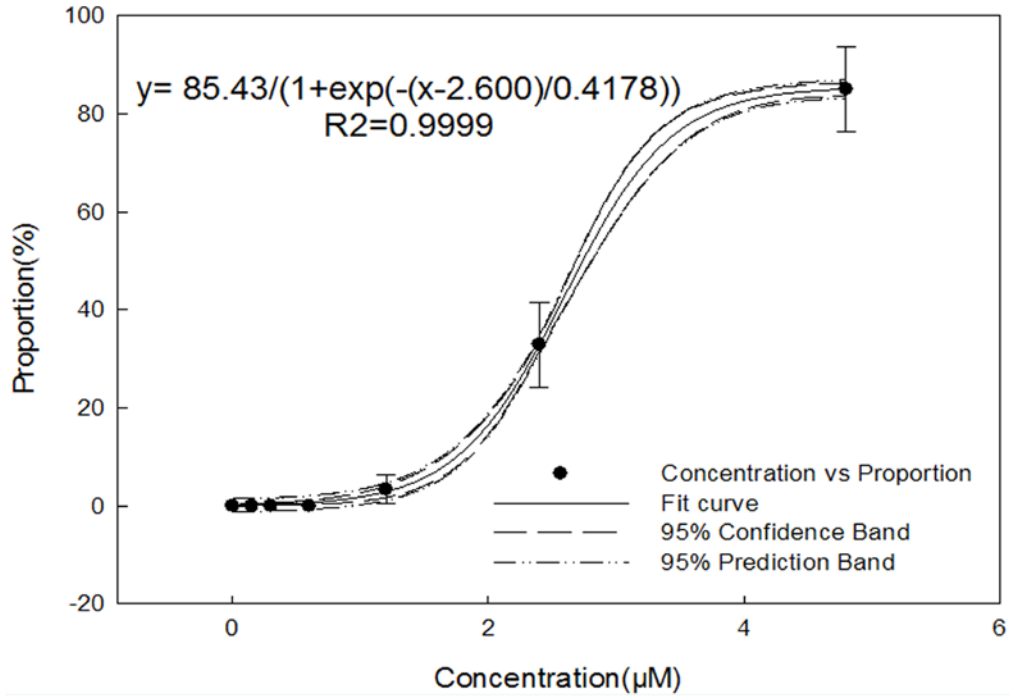


Figure S3. S-Curve of abnormalities 74 hpf resulted from TBBPA, $LC_{50}=2.38 \mu\text{M}$ ($1.3 \times 10^3 \mu\text{g/L}$), Transformation of the internal dose was $21.66 \mu\text{g/g}$.

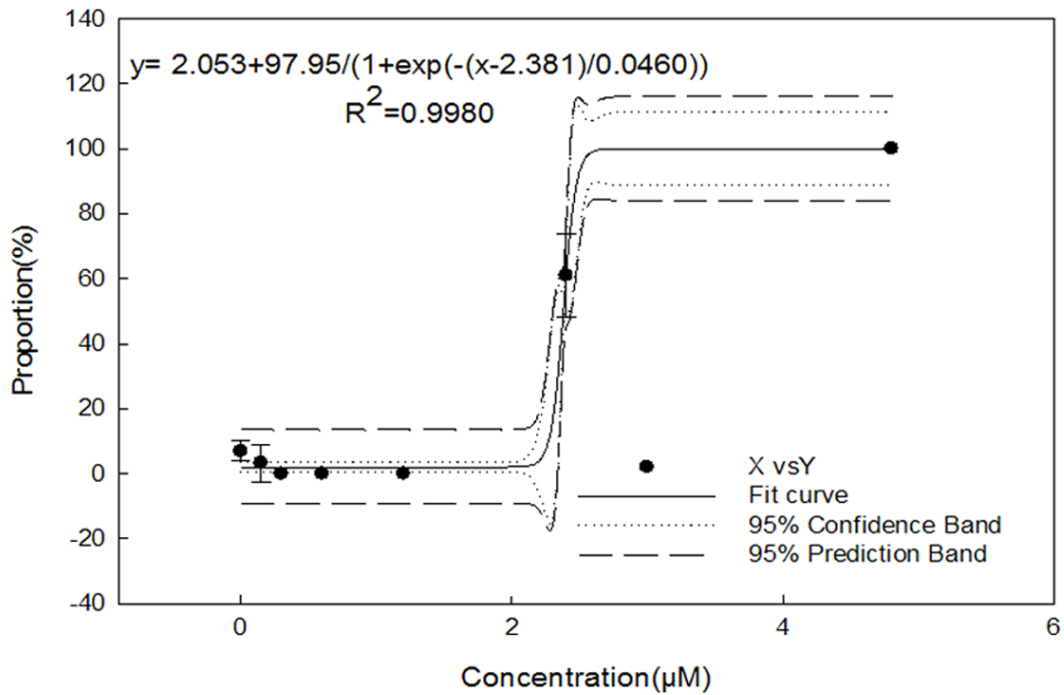
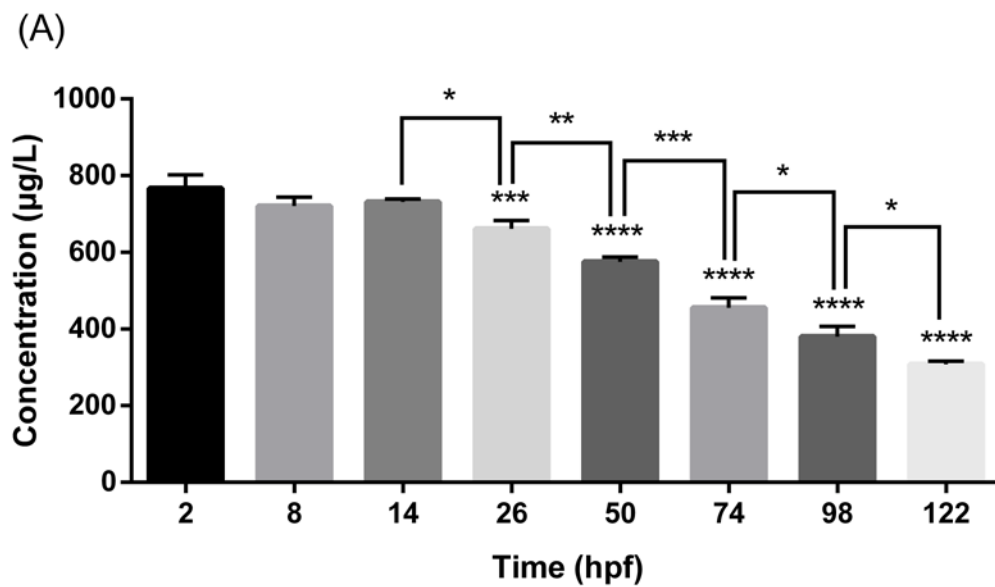


Figure S4. The results of the multiple comparisons of ordinary one-way ANOVA. Measured concentrations of TBBPA in exposure medium ($\mu\text{g/L}$) (**A**) and in zebrafish embryos/larvae (ng/g, wm) (**B**) across early life-stages (hpf). Asterisk on the error bar represent the significant difference compared with initial groups while asterisk on the each striping represnet the significant difference between each two columns.* represent $p<0.05$; ** represent $p<0.01$; *** represent $p<0.001$ and **** represent $p<0.0001$, respectively.



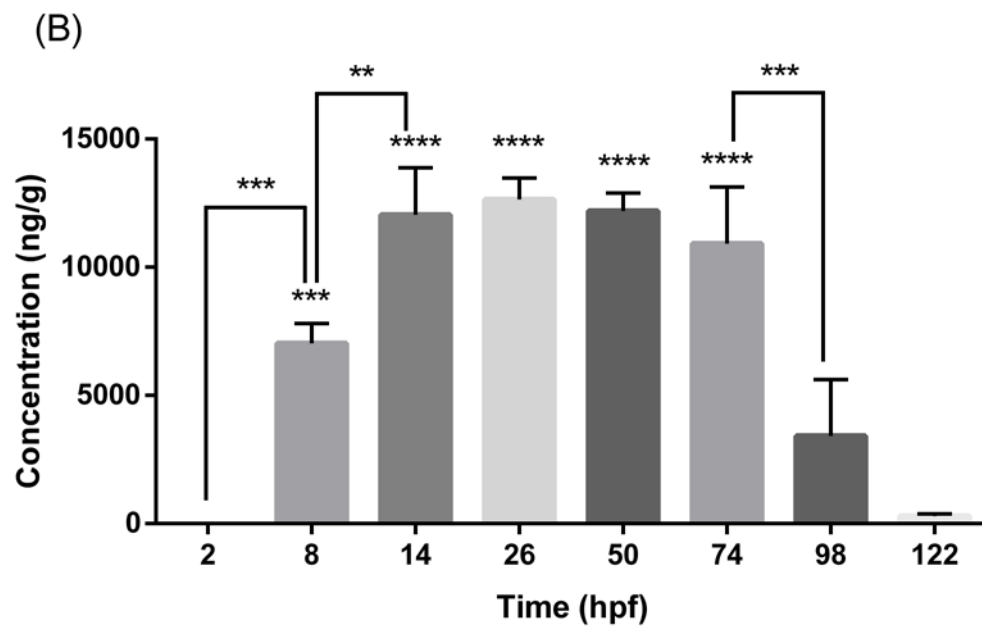
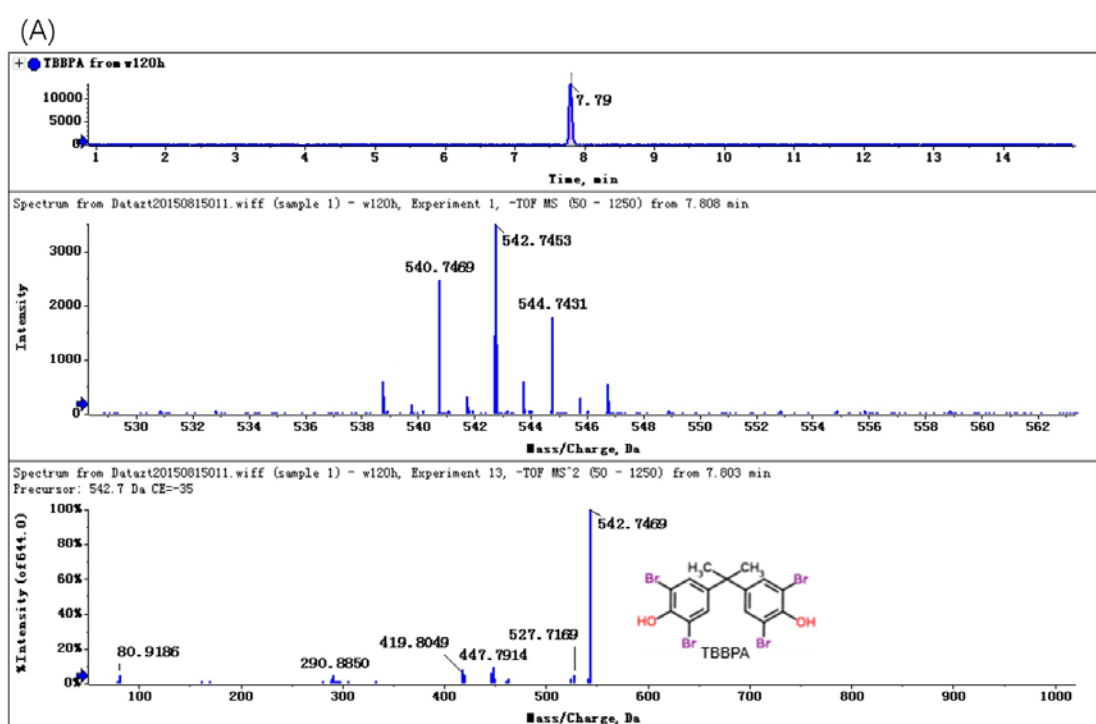
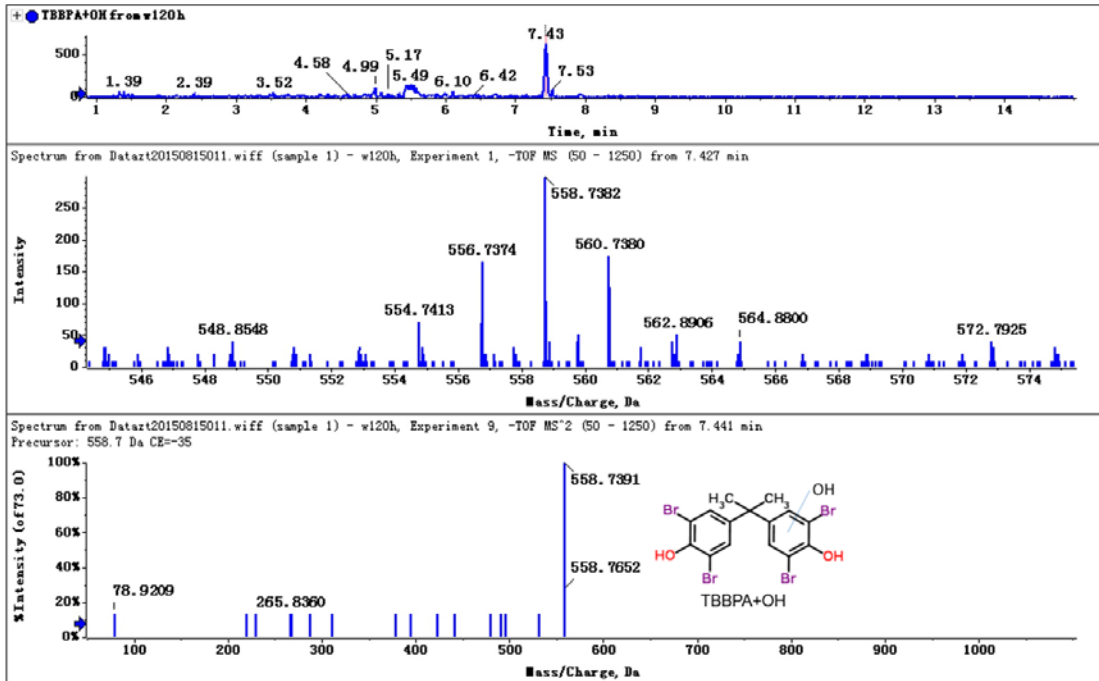


Figure S5. Mass spectrum and secondary spectrum diagram of the parent TBBPA and its metabolites in solution or larvae body at 120 hpf. **(A)** Parent TBBPA, **(B)** TBBPA-hydroxylated (TBBPA+OH), **(C)** TBBPA-monosulfate (TBBPA+SO₃H), **(D)** methoxylated 2,6-dibromo-4-isopropyl-phenol (TBBPA-Ph+CH₂OH) and **(E)** hydroxylated 2,6-dibromo-4-isopropyl-phenol (TBBPA-Ph+OH) formed by oxidative cleavage from TBBPA. Ph=C₆H₃OBr₂

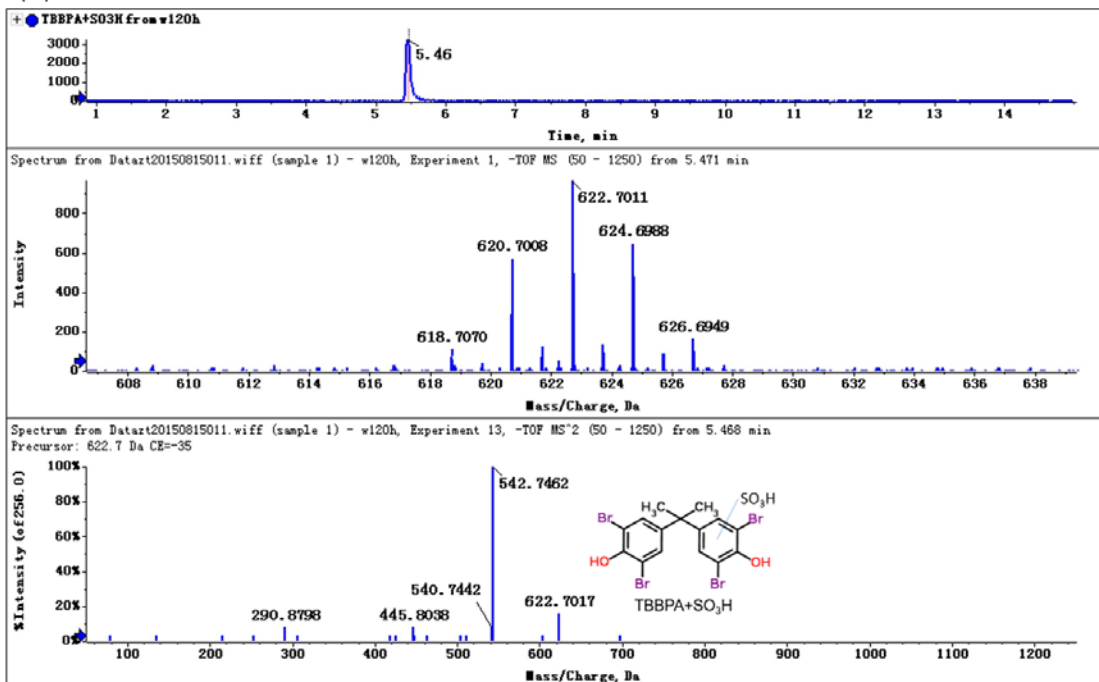


2016/1/26 15:12:11

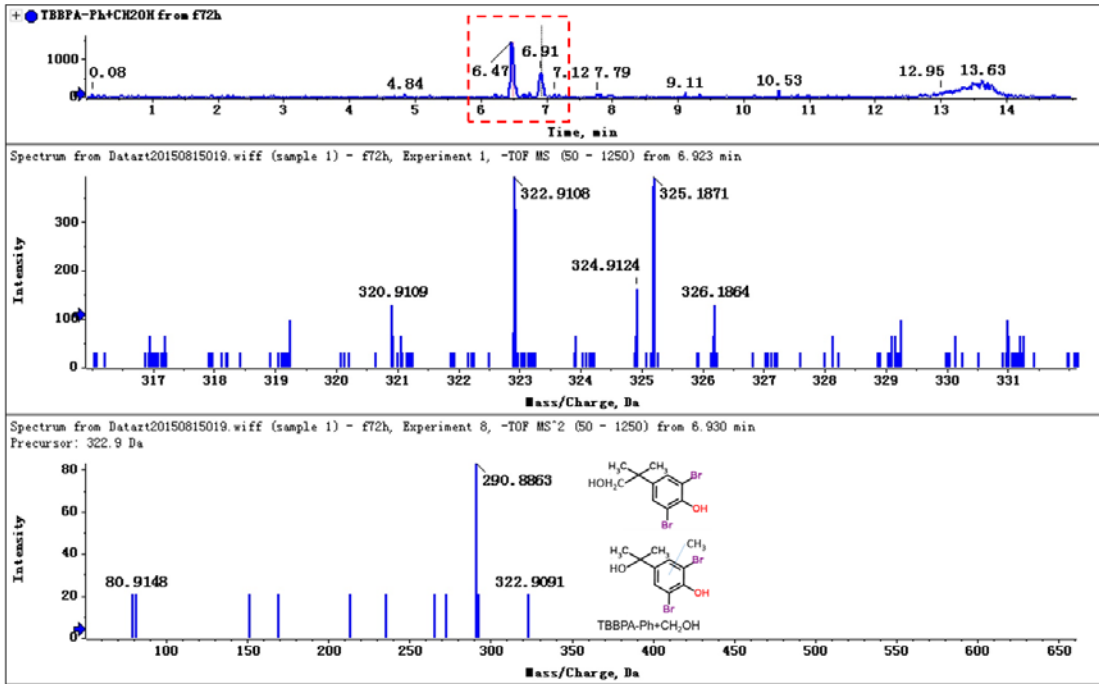
(B)



(C)



(D)



(E)

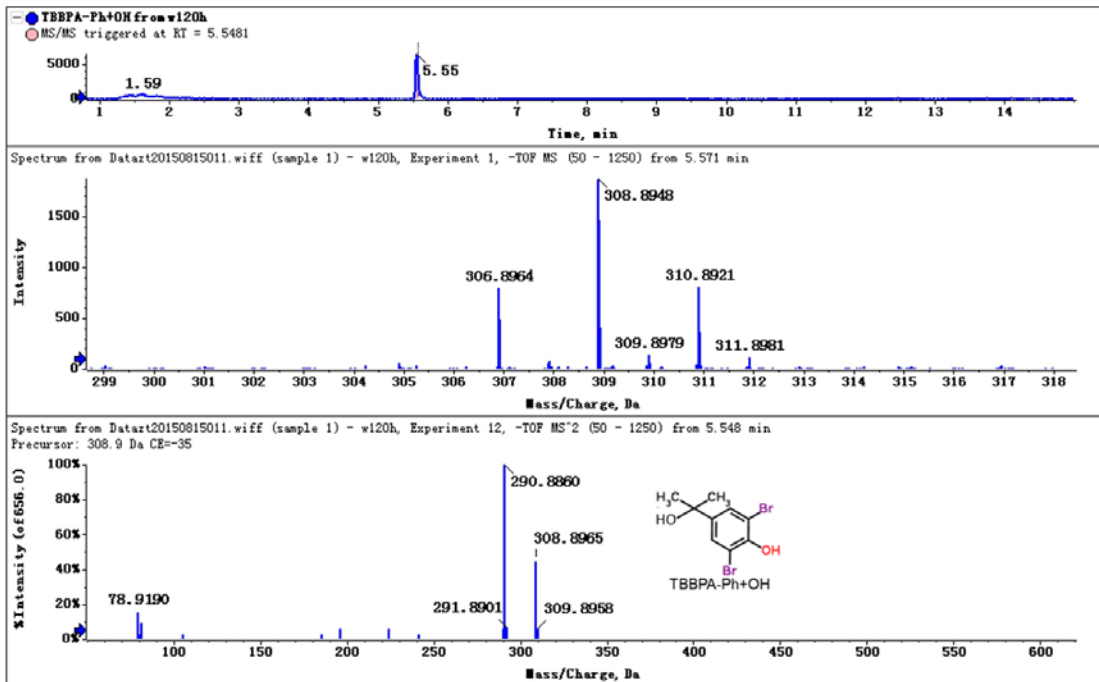


Table S1. Optimized instrumental parameters, multiple reaction monitoring (MRM; mass-to-charge (m/z)) transitions and limit of quantification (LOQ) for TBBPA analyzed by liquid chromatography–electrospray ionization (-)-tandem mass spectrometry.

Compound	Rt (min)	Precursor ion (m/z)	Quantification			Confirmation			Linearity, R2 (0.1-100 μg/L)	LOD (μg/L, ng/g)
			Q3	Declustering potential (v)	Collision energy (eV)	Q3	Declustering potential (v)	Collision energy (eV)		
TBBPA	9.21	543.0[M-H]-	417.8	-125	-58	291	-125	-49	0.9985	0.04, 0.34

Table S2. Raw data of TBBPA in exposure water by HPLC-QTRAP.

Index	Sample Name	Exposure Time/hpf	Component Name	Area	Height	Retention Time	Width at 50%	Water concentration $\mu\text{g/L}$	Average $\mu\text{g/L}$
1	w-0-1	2	543.0 / 417.8	6.7×10^5	7.2×10^4	9.2	1.4×10^{-1}	7.5×10^2	7.7×10^2
2	w-0-2	2	543.0 / 417.8	6.6×10^5	7.1×10^4	9.2	1.4×10^{-1}	7.4×10^2	
3	w-0-3	2	543.0 / 417.8	7.2×10^5	7.8×10^4	9.2	1.4×10^{-1}	8.1×10^2	
4	w-6-1	8	543.0 / 417.8	6.2×10^5	6.7×10^4	9.2	1.4×10^{-1}	7.0×10^2	7.2×10^2
5	w-6-2	8	543.0 / 417.8	6.3×10^5	7.0×10^4	9.2	1.4×10^{-1}	7.1×10^2	
6	w-6-3	8	543.0 / 417.8	6.6×10^5	7.3×10^4	9.2	1.4×10^{-1}	7.5×10^2	
7	w-12-1	14	543.0 / 417.8	6.5×10^5	6.9×10^4	9.2	1.4×10^{-1}	7.4×10^2	7.3×10^2
8	w-12-2	14	543.0 / 417.8	6.5×10^5	7.0×10^4	9.2	1.4×10^{-1}	7.4×10^2	
9	w-12-3	14	543.0 / 417.8	6.4×10^5	7.0×10^4	9.2	1.4×10^{-1}	7.2×10^2	
10	w-24-1	26	543.0 / 417.8	5.9×10^5	6.4×10^4	9.2	1.4×10^{-1}	6.6×10^2	6.6×10^2
11	w-24-2	26	543.0 / 417.8	6.1×10^5	6.6×10^4	9.2	1.4×10^{-1}	6.8×10^2	
12	w-24-3	26	543.0 / 417.8	5.7×10^5	6.2×10^4	9.2	1.4×10^{-1}	6.4×10^2	
13	w-48-1	50	543.0 / 417.8	5.1×10^5	5.8×10^4	9.2	1.3×10^{-1}	5.7×10^2	5.8×10^2
14	w-48-2	50	543.0 / 417.8	5.2×10^5	5.8×10^4	9.2	1.4×10^{-1}	5.9×10^2	

15	w-48-3	50	543.0 / 417.8	5.0×10^5	5.5×10^4	9.2	1.4×10^{-1}	5.6×10^2	
16	w-72-1	74	543.0 / 417.8	4.2×10^5	4.6×10^4	9.2	1.3×10^{-1}	4.7×10^2	4.6×10^2
17	w-72-2	74	543.0 / 417.8	4.2×10^5	4.7×10^4	9.2	1.4×10^{-1}	4.7×10^2	
18	w-72-3	74	543.0 / 417.8	3.8×10^5	4.2×10^4	9.2	1.4×10^{-1}	4.3×10^2	
19	w-96-1	98	543.0 / 417.8	3.3×10^5	4.2×10^4	9.2	1.2×10^{-1}	3.7×10^2	3.8×10^2
20	w-96-2	98	543.0 / 417.8	3.6×10^5	4.3×10^4	9.2	1.3×10^{-1}	4.1×10^2	
21	w-96-3	98	543.0 / 417.8	3.2×10^5	3.8×10^4	9.2	1.2×10^{-1}	3.6×10^2	
22	w-120-1	122	543.0 / 417.8	2.7×10^5	3.1×10^4	9.2	1.3×10^{-1}	3.0×10^2	3.1×10^2
23	w-120-2	122	543.0 / 417.8	2.7×10^5	3.1×10^4	9.2	1.3×10^{-1}	3.0×10^2	
24	w-120-3	122	543.0 / 417.8	2.8×10^5	3.3×10^4	9.2	1.2×10^{-1}	3.2×10^2	

Table S3. Raw data of TBBPA in zebrafish Embryos /Larvae by HPLC-QTRAP.

Index	Sample Name	Exposure Time/hpf	Component Name	Area	Height	Retention Time	Width at 50%	Embryos /Larvae Concentration $\mu\text{g/L}$	Average Conc	Embryos /Larvae Average Mass/g	Numbers of Embryos	Total mass/g	Zfish/ ng/g (wet mass)	Average Concentration in Zfish/ ng/g (wet mass)
1	f-0-1	2	543.0 / 417.8	1.17×10^3	2.30×10^2	9.12	0.10	ND	ND	7.7×10^{-4}	15	0.01	ND	ND
2	f-0-2	2	543.0 / 417.8	1.20×10^4	1.97×10^3	9.13	0.10	ND		7.7×10^{-4}	15	0.01	ND	
3	f-0-3	2	543.0 / 417.8	5.85×10^3	8.90×10^2	9.13	0.11	ND		7.7×10^{-4}	15	0.01	ND	
4	f-6-1	8	543.0 / 417.8	1.79×10^5	2.27×10^4	9.14	0.12	79.32	10.98	7.7×10^{-4}	15	0.01	6.9×10^3	7.0×10^3
5	f-6-2	8	543.0 / 417.8	1.66×10^5	2.16×10^4	9.15	0.12	73.30		7.7×10^{-4}	15	0.01	6.3×10^3	
6	f-6-3	8	543.0 / 417.8	2.05×10^5	2.50×10^4	9.14	0.12	90.99		7.7×10^{-4}	15	0.01	7.9×10^3	
7	f-12-1	14	543.0 / 417.8	2.85×10^5	3.82×10^4	9.14	0.12	127.59	11.98	7.7×10^{-4}	12	0.01	1.4×10^4	1.2×10^4
8	f-12-2	14	543.0 / 417.8	2.52×10^5	3.13×10^4	9.14	0.12	112.46		7.7×10^{-4}	12	0.01	1.2×10^4	
9	f-12-3	14	543.0 / 417.8	2.45×10^5	3.29×10^4	9.14	0.12	109.38		7.7×10^{-4}	14	0.01	1.0×10^4	
10	f-24-1	26	543.0 / 417.8	3.08×10^5	3.94×10^4	9.14	0.12	137.86	12.98	7.7×10^{-4}	14	0.01	1.3×10^4	1.3×10^4
11	f-24-2	26	543.0 / 417.8	4.13×10^5	5.36×10^4	9.14	0.12	185.65		7.7×10^{-4}	18	0.01	1×10^4	

12	f-24-3	26	543.0 / 417.8	3.63×10^5	4.76×10^4	9.15	0.11	162.84		7.7×10^{-4}	18.	0.01	1.2×10^4	
13	f-48-1	50	543.0 / 417.8	2.91×10^5	3.81×10^4	9.13	0.12	130.15	13.98	7.7×10^{-4}	13	0.01	1.3×10^4	1.2×10^6
14	f-48-2	50	543.0 / 417.8	3.04×10^5	4.06×10^4	9.14	0.11	136.07		7.7×10^{-4}	15	0.01	1.2×10^4	
15	f-48-3	50	543.0 / 417.8	3.04×10^5	3.99×10^4	9.15	0.12	136.32		7.7×10^{-4}	15	0.01	1.2×10^4	
16	f-72-1	74	543.0 / 417.8	2.80×10^5	3.61×10^4	9.14	0.12	125.26	14.98	7.7×10^{-4}	17.	0.01	9.57×10^3	1.09×10^4
17	f-72-2	74	543.0 / 417.8	3.24×10^5	3.98×10^4	9.14	0.13	145.24		7.7×10^{-4}	14	0.01	1.35×10^4	
18	f-72-3	74	543.0 / 417.8	2.68×10^5	3.51×10^4	9.13	0.12	119.57		7.7×10^{-4}	16	0.01	9.71×10^3	
19	f-96-1	98	543.0 / 417.8	1.36×10^5	1.90×10^4	9.13	0.11	59.97	15.98	7.7×10^{-4}	15	0.01	5.19×10^3	3.42×10^3
20	f-96-2	98	543.0 / 417.8	9.48×10^4	1.26×10^4	9.13	0.11	41.07		7.7×10^{-4}	13	0.01	4.10×10^3	
21	f-96-3	98	543.0 / 417.8	3.25×10^4	4.51×10^3	9.14	0.11	12.73		7.7×10^{-4}	17	0.01	9.72×10^2	
22	f-120-1	122	543.0 / 417.8	1.59×10^4	2.23×10^3	9.14	0.11	5.20	16.98	7.7×10^{-4}	17	0.01	3.97×10^2	2.93×10^2
23	f-120-2	122	543.0 / 417.8	1.08×10^4	1.60×10^3	9.13	0.10	2.90		7.7×10^{-4}	15	0.01	2.51×10^2	
24	f-120-3	122	543.0 / 417.8	9.96×10^3	1.46×10^3	9.12	0.11	2.50		7.7×10^{-4}	14	0.01	2.31×10^2	

Table S4. Raw data of TBBPA and metabolites in exposure water and zebrafish body by HPLC-TripleTOF.

In solution:

Compound Name	Formula	m/z	Found RT (min)
TBBPA	C15H12Br4O2	538.7498	7.79
TBBPA+OH	C15H12Br4O3	554.7447	7.43
TBBPA+SO3H	C15H12Br4O5S	618.7066	5.45
TBBPA-Ph*+CH2OH	C10H12Br2O2	320.9131	6.50
TBBPA-Ph+OH	C9H10Br2O2	306.8975	5.55

WATER														
Area									concentration (µg/L)					
	TBBPA	TBBPA+OH	TBBPA+SO3H	TBBPA-Ph+CH2OH	TBBPA-Ph+OH	1+3	1+2+3	1+2+3+4+5	time (hpf)	TBBPA	TBBPA+OH	TBBPA+SO3H	TBBPA-Ph+OH	SUM
2	131450.0664	1509.600489	n. d.	140866.95	53871.53695	131450.0664	132959.6669	327698.1539	2	767.1837776	8.810501488	n. d.	n. d.	775.9942791
8	111693.322	1757.234636	n. d.	121671.674	51291.33161	111693.322	113450.5566	286413.5622	8	720.5141332	11.33561406	n. d.	n. d.	731.8497473
14	138989.6928	1795.142674	n. d.	132754.9081	56639.99184	138989.6928	140784.8355	330179.7355	14	731.0857462	9.442449971	n. d.	28.13395132	768.6621475
26	117418.5645	1606.82455	n. d.	123659.7172	57690.23688	117418.5645	119025.3891	300375.3432	26	661.1103592	9.04702216	n. d.	5.913271739	676.0706531
50	126922.2979	2546.047604	n. d.	92866.0385	62759.58223	126922.2979	129468.3455	285093.9662	50	575.3417867	11.54129418	n. d.	22.97946268	609.8625436
74	121654.3948	2748.912803	1584.813597	74756.16611	59400.80823	123239.2084	125988.1212	260145.0956	74	455.5257073	10.29309669	5.934215	n. d.	471.753019

98	103478.7211	3088.509167	12794.93526	57986.70369	66422.88613	116273.6563	119362.1655	243771.7553	98	380.5786672	11.35905711	47.05778499	25.8261121	464.8216214
122	74110.35537	3588.03666	29748.62634	40518.60068	69394.94256	103858.9817	107447.0184	217360.5616	122	307.5017707	14.88763103	123.4342384	12.33178021	458.1554204

In zebrafish body:

Compound Name	Formula	m/z	Found RT (min)
TBBPA	C15H12Br4O2	538.7498	7.79
TBBPA-Ph+CH ₂ OH	C10H12Br2O2	320.9131	6.50
TBBPA-Ph+CH ₂ OH	C10H12Br2O2	320.9131	6.92
TBBPA-Ph+OH	C9H10Br2O2	306.8975	5.55

FISH															
Area								concentration (ng/g)							
	TBBPA	TBBPA+OH	TBBPA+SO3	TBBPA-Ph+CH2OH	TBBPA-Ph+OH	TBBPA-Ph+CH2OH (RT6.92)	2+3+4	time (hr)	TBBPA	TBBPA+OH	TBBPA+SO3	TBBPA-Ph+CH2OH	TBBPA-Ph+OH	TBBPA-Ph+CH2OH (RT6.92)	SUM
2	23570.98571	n. d.	n. d.	3646.6807	1538.550969	n. d.	5185.231669	2	0.86387151	n. d.	n. d.	0.133650056	0.056387559	n. d.	1.053909125
8	164661.734	n. d.	n. d.	11053.24991	1974.1962	3802.090208	16829.53632	8	7.030483456	n. d.	n. d.	0.471935335	0.084291313	0.162336031	7.749046135
14	276307.431	n. d.	n. d.	15943.08782	9053.076558	7213.452519	32209.6169	14	12.04229354	n. d.	n. d.	0.694846833	0.394559802	0.314383556	13.44608373
26	218114.9162	n. d.	n. d.	17032.68048	5986.262544	8650.038036	31668.98106	26	12.64391124	n. d.	n. d.	0.987368053	0.347017864	0.501434359	14.47973152
50	338463.5034	n. d.	n. d.	24730.15008	6193.361819	8793.521229	39717.03313	50	12.19510237	n. d.	n. d.	0.891046476	0.223151627	0.316837386	13.62613786
74	314838.4837	n. d.	n. d.	13378.21491	1110.050377	7912.414487	22400.67978	74	10.91604139	n. d.	n. d.	0.463847831	0.038487531	0.274338267	11.69271502

98	153227.1211	n. d.	n. d.	10930.54827	3431.219035	3938.617572	18300.38488	98	3.422632724	n. d.	n. d.	0.244155551	0.076643106	0.087976863	3.831408244
122	15700.76028	n. d.	n. d.	6013.409479	1644.51696	655.4605547	8313.386994	122	0.293174391	n. d.	n. d.	0.112286133	0.030707447	0.012239168	0.44840714

Table S5. Using ECOSAR to estimate the acute toxicity value (LC₅₀ at 96 hpf) of TBBPA and metabolites.

Name ^a	SMILES	ECOSAR Class	Organism	Duration	End Pt	Predicted mg/L (ppm)	Relative Potency	Cumulative Conc (µg/L) ^b	TU
TBBPA	<chem>C2=C(Br)C(O)=C(Br)C=C2C(C)(C)C1=CC(Br)=C(O)C(Br)=C1</chem>	Phenols, Poly	Fish	96-hr	LC ₅₀	0.023	1.0	1.09E+04	148.81
TBBPA+OH	<chem>C2(O)=C(Br)C(O)=C(Br)C=C2C(C)(C)C1=CC(Br)=C(O)C(Br)=C1</chem>	Phenols, Poly	Fish	96-hr	LC ₅₀	0.046	2.0	1.01E+03	0.0074
TBBPA+SO ₃ H	<chem>C2=C(Br)C(OS(=O)(=O)O)=C(Br)C=C2C(C)(C)C1=CC(Br)=C(O)C(Br)=C1</chem>	Phenols	Fish	96-hr	LC ₅₀	0.933	40.6	7.84E+02	0.0004
TBBPA-Ph+CH ₂ OH	<chem>C1=C(Br)C(O)=C(Br)C=C1C(C)(C)CO</chem>	Phenols	Fish	96-hr	LC ₅₀	2.69	106.0	7.21E-01	0.091
TBBPA-Ph+CH ₂ OH (RT=6.92)	<chem>C1=C(Br)C(O)=C(Br)C(C)=C1C(C)(C)O</chem>	Phenols	Fish	96-hr	LC ₅₀	2.438	117.0	3.17E-01	0.036
TBBPA-Ph+OH	<chem>C1=C(Br)C(O)=C(Br)C=C1C(O)(C)C</chem>	Phenols	Fish	96-hr	LC ₅₀	6.078	264.3	2.14E-01	0.013

^a Ph=C₆H₃OBr₂, 2,6-dibromo-4-isopropyl-phenol

^b Cumulative residual dose unit (ng/g) in zebrafish larvae have been converted into concentration unit (µg/L)

Table S6. Primer Sequences of receptor-associated genes among ThR, AR, ER and AhR receptors for qRT-PCR.

Gene name	Forward Primer (5'-3')	Reverse Primer (5'-3')	Accession number
<i>β-actin</i>	tggtattgtgatggactctg	attgccgatggtgatgac	AF057040
<i>ahr1a</i>	ctacagccacctccatac	accttctcagccggtat	NM_131028
<i>ahr1b</i>	ggagagcacttgaggaaacg	ggatccagatcgcctttga	NM_001024816
<i>ahr2</i>	atctccatgggcaaaacaag	tcctcttgtgtcgataccc	NM_131264
<i>Ahrra</i>	gctgctgatgtttggactga	gacgctgtgttcacgtcact	NM_001035265
<i>Ahrrb</i>	acctgggatttcatcagacg	gctgtacagatgagccgtca	NM_001033920
<i>Ar</i>	acattctggaggccattgag	acgtgcaagttacggaaacc	NM_001083123
<i>arnt2</i>	gaatggtctcgggccgtcta	agctggtcacctgcagtctt	NM_131674
<i>arntl1a</i>	tctctgggggaaagaagat	ccatcgctgcttcatcatta	NM_131577
<i>arntl1b</i>	ctcgctgaatgccatagaca	cccagagacactgtattggt	NM_178300
<i>c1d</i>	acggagagctgacagacat	gccgacatcagatccagttt	NM_001007059
<i>ccnd1</i>	tgacttgccctgacttgtcg	gaaaaagcagggagcacttg	NM_131025
<i>ctnbl</i>	atcctgtccaacctgacctg	tctctgcatcctggtgtctg	NM_131059
<i>cyp19b</i>	ggcagtctctggaggatgac	cagtgttctcgaagttctcca	AY780257
<i>er1</i>	ggtccagtgtggtgtcctct	cacacgaccagactccgtaa	NM_152959
<i>er2a</i>	agcttgtgcacatgatcagc	gctttcatccctgctgagac	NM_180966
<i>er2b</i>	ttgtgttctccagcatgagc	ccacatatggggaaggaatg	NM_174862
<i>hdac3</i>	agccatgaaggtgtccattc	agaagctgcttgaggactc	NM_200990
<i>ncoa1</i>	tgagagcctctgttgaggt	ctctgaccctggtttggtgt	XM_686652
<i>ncoa2</i>	agagcctgtcagtcccaaga	ggctgtagccaccatcagtt	NM_131777
<i>ncoa3</i>	aactcacctgccacaaatc	agaggcctgttctgtgctta	XM_687846
<i>ncoa4</i>	gacaactcgggaaagaagc	ctggggatttggcagagtta	NM_201129
<i>ncor1</i>	agggtaaggagcagagcaca	gcaaaactggttcaggtggt	EF016488
<i>ncor2</i>	ttgaaccagtttaccacca	tgacaatggctgagttgctc	NM_001007032
<i>pa2g4a</i>	cgggaaaaggacatgaagaa	aagccgtcaacatgaactcc	NM_001002170
<i>pa2g4b</i>	caaagacaccaccagtttg	gtgccaccattacgctttt	NM_212641
<i>Pgr</i>	caacaggtggttggacag	atgtggagatgtccgctttg	NM_001166335
<i>sp1</i>	tcctccattaatcggtcgag	tgtgtgtgagcaciaaacga	NM_212662
<i>Thra</i>	caatgtaccatttcgcttg	gctcctgctctgttttcc	NM_131396
<i>vtg1</i>	ctgctggaagttgcatgct	gaccagcattgcccataact	NM_001044897
<i>vtg2</i>	tactttgggactgatgcaa	agacttcgtgaagcccaaga	AY729644

Table S7. Fold-change of gene expressions in NR pathways, *p<0.05, **p<0.01 indicates significant difference between exposure groups and the control.

TBBPA				TBBPA			
<i>gene</i>	Con($\mu\text{g/L}$)	Mean	SD	<i>gene</i>	Con($\mu\text{g/L}$)	Mean	SD
<i>ahr1a</i>	0	-1.00	0.26	<i>ahr1b</i>	0	-1.00	0.28
	1.6×10^2	-1.42	0.38		1.6×10^2	-1.06	0.24
	3.3×10^2	-2.04	0.14		3.3×10^2	-1.33	0.30
	6.5×10^2	-1.50	0.11		6.5×10^2	-1.11	0.34
<i>ahr2</i>	0	-1.00	0.45	<i>ahrra</i>	0	-1.00	0.54
	1.6×10^2	-2.41	0.12		1.6×10^2	-2.36	0.12
	3.3×10^2	-2.20	0.20		3.3×10^2	-2.34	0.25
	6.5×10^2	-2.28	0.23		6.5×10^2	-2.13	0.20
<i>ahrrb</i>	0	-1.00	0.46	<i>ar</i>	0	-1.00	0.36
	1.6×10^2	-1.62	0.29		1.6×10^2	-1.93*	0.20
	3.3×10^2	-3.26	0.14		3.3×10^2	-3.14**	0.04
	6.5×10^2	-2.71	0.19		6.5×10^2	-1.89*	0.18
<i>arnt2</i>	0	-1.00	0.52	<i>arnt1a</i>	0	-1.00	0.22
	1.6×10^2	-1.80	0.36		1.6×10^2	-1.45	0.10
	3.3×10^2	-3.49	0.11		3.3×10^2	-1.29	0.10
	6.5×10^2	-2.08	0.11		6.5×10^2	-1.37	0.12
<i>arnt1b</i>	0	-1.00	0.37	<i>cld</i>	0	-1.00	0.09
	1.6×10^2	-1.40	0.37		1.6×10^2	-1.31	0.34
	3.3×10^2	-1.56	0.35		3.3×10^2	-1.20	0.45
	6.5×10^2	-1.92	0.07		6.5×10^2	-2.87*	0.11
<i>ccnd1</i>	0	-1.00	0.22	<i>ctnbl</i>	0	-1.00	0.31
	1.6×10^2	-2.50**	0.17		1.6×10^2	-2.31	0.20
	3.3×10^2	-2.73**	0.20		3.3×10^2	-1.92	0.19
	6.5×10^2	-2.04*	0.09		6.5×10^2	-1.29	0.40
<i>cyp19b</i>	0	-1.00	0.53	<i>erl</i>	0	-1.00	0.45

	1.6×10^2	-1.55	0.35		1.6×10^2	-2.10	0.12
	3.3×10^2	-1.56	0.65		3.3×10^2	-1.08	1.13
	6.5×10^2	-1.58	0.25		6.5×10^2	-2.42	0.09
<i>er2a</i>	0	-1.00	0.41	<i>er2b</i>	0	-1.00	0.41
	1.6×10^2	-1.84*	0.03		1.6×10^2	-2.09	0.14
	3.3×10^2	-3.23**	0.14		3.3×10^2	-2.25*	0.34
	6.5×10^2	-2.55*	0.15		6.5×10^2	-2.49*	0.08
<i>hdac3</i>	0	-1.00	0.11	<i>ncoa1</i>	0	-1.00	1.01
	1.6×10^2	-1.44	0.41		1.6×10^2	-1.40	0.42
	3.3×10^2	-1.54	0.30		3.3×10^2	-3.47	0.23
	6.5×10^2	-1.36	0.32		6.5×10^2	-3.54	0.09
<i>ncoa2</i>	0	-1.00	0.22	<i>ncoa3</i>	0	-1.00	0.42
	1.6×10^2	-1.75*	0.15		1.6×10^2	-2.55*	0.10
	3.3×10^2	-2.47**	0.13		3.3×10^2	-1.15	0.31
	6.5×10^2	-2.10**	0.14		6.5×10^2	-1.75	0.23
<i>ncoa4</i>	0	-1.00	0.16	<i>ncor1</i>	0	-1.00	0.09
	1.6×10^2	-1.68**	0.05		1.6×10^2	-1.43	0.25
	3.3×10^2	-1.90***	0.05		3.3×10^2	-1.73*	0.31
	6.5×10^2	-1.35*	0.01		6.5×10^2	-1.65	0.11
<i>ncor2</i>	0	-1.00	0.12	<i>pa2g4b</i>	0	-1.00	0.26
	1.6×10^2	-1.94	0.30		1.6×10^2	-1.15	0.08
	3.3×10^2	-1.78	0.15		3.3×10^2	-1.27	0.25
	6.5×10^2	-1.77	0.17		6.5×10^2	-1.12	0.07
<i>pgr</i>	0	-1.00	0.56	<i>sp1</i>	0	-1.00	0.22
	1.6×10^2	-2.15	0.18		1.6×10^2	-1.51	0.12
	3.3×10^2	-1.27	0.69		3.3×10^2	-1.53	0.25
	6.5×10^2	-2.58	0.24		6.5×10^2	-1.52	0.05
<i>thra</i>	0	-1.00	0.08	<i>vtg1</i>	0	-1.00	0.28
	1.6×10^2	-1.47*	0.30		1.6×10^2	-1.74	0.24
	3.3×10^2	-2.35**	0.12		3.3×10^2	-1.44	0.63
	6.5×10^2	-1.51*	0.04		6.5×10^2	-2.32	0.18
<i>vtg2</i>	0	-1.00	0.51	<i>vtg4</i>	0	-1.00	0.51

	1.6×10^2	-1.49	0.25		1.6×10^2	-1.33	0.37
	3.3×10^2	-1.18	0.88		3.3×10^2	-1.40	0.73
	6.5×10^2	-2.05	0.26		6.5×10^2	-1.97	0.28